Does reptation describe the dynamics of entangled, finite length polymer systems? A model simulation

Andrzej Kolinski,[a] Jeffrey Skolnick,[b] and Robert Yaris
Department of Chemistry, Institute of Macromolecular Chemistry, Washington University, St. Louis, Missouri 63130

(Received 8 September 1986; accepted 16 October 1986)

In order to examine the validity of the reptation model of motion in a dense collection of polymers, dynamic Monte Carlo (MC) simulations of polymer chains composed of n beads confined to a diamond lattice were undertaken as a function of polymer concentration ϕ and degree of polymerization n. We demonstrate that over a wide density range these systems exhibit the experimentally required molecular weight dependence of the center-of-mass self-diffusion coefficient $D \sim n^{-2.1}$ and the terminal relaxation time of the end-to-end vector $\tau_R \sim n^{3.4}$. Thus, these systems should represent a highly entangled collection of polymers appropriate to look for the existence of reptation. The time dependence of the average single bead mean-square displacement, as well as the dependence of the single bead displacement on position in the chain were examined, along with the time dependence of the center-of-mass displacement. Furthermore, to determine where in fact a well-defined tube exists, the mean-square displacements of a polymer chain down and perpendicular to its primitive path defined at zero time were calculated, and snapshots of the primitive path as a function of time are presented. For an environment where all the chains move, no evidence of a tube, whose existence is central to the validity of the reptation model, was found. However, if a single chain is allowed to move in a partially frozen matrix of chains (where all chains but one are pinned every n_e beads, and where between pin points the other chains are free to move), reptation with tube leakage is recovered for the single mobile chain. The dynamics of these chains possesses aspects of Rouse-like motion; however, unlike a Rouse chain, these chains undergo highly cooperative motion that appears to involve a backflow between chains to conserve constant average density. While these simulations cannot preclude the onset of reptation at higher molecular weight, they strongly argue at a minimum for the existence with increasing n of a crossover regime from simple Rouse dynamics in which reptation plays a minor role at best.

I. INTRODUCTION

Over the past ten years or so, it has become widely accepted that the reptation model successfully describes the dynamics of polymer chains in the melt or in concentrated solutions.[1,2] A description of which kinds of motion of the chains in a dense medium lead to the macroscopically measurable properties of diffusion and viscosity is complicated, when compared to that in dilute solution, by the mutual entanglements of the various chains.[3,4] The reptation model attacks the role of interchain entanglements in a direct way and postulates (in its simplest form—see below) that the dynamics of each chain in the melt is equivalent to the situation where, as schematically depicted in Fig. 1, the entanglements due to the neighboring chains act to effectively confine the chain of interest to a tube of diameter d_T. Thus, in the context of this mean field treatment, an effective separation of time scales is assumed between the dynamics of the test chain and the entanglements that define the location of its tube. The constraints due to the tube insure that the dominant motion of each chain is a "slithering" motion down the chain, hence the name "reptation." The reptation model has been quite successful in rationalizing the measured molecular weight dependence of the center-of-mass diffusion coefficient and the low frequency shear viscosity coefficient.[5,6]

In this paper, we construct a simplified model of the dynamics of densely packed and entangled polymer chains, which we can follow for a long time by a dynamic Monte Carlo (MC) simulation.[7] The major purpose of this simulation, which should be thought of as a computational experiment, is to investigate whether the basic assumption of reptation holds—that the dominant motion of each chain is a slithering motion in a tube arising from entanglements. This paper continues our recently published work where we reported the results of a Monte Carlo simulation of the dynamics of a multichain system confined to a diamond lattice which represents a model of a polymer melt or a very concentrated polymer solution.[8] We showed that over a wide concentration range, up to volume fraction of polymer ϕ equal to 0.857, the correlated short time and distance motion of the system can be satisfactorily described in terms of the cooperative migration of conformational "defects" moving mostly in a direction perpendicular to the local orientation of the chain backbone. We observed that the mean-square displacement of a single monomer $g(t)$ exhibited three well-defined regimes for distances of displacement below the radius of gyration of a chain. On a distance scale comparable to

[a] Permanent address: Department of Chemistry, University of Warsaw, 02-093 Warsaw, Poland.
[b] Alfred P. Sloan Foundation Fellow.

 0021-9606/87/031567-19$02.10

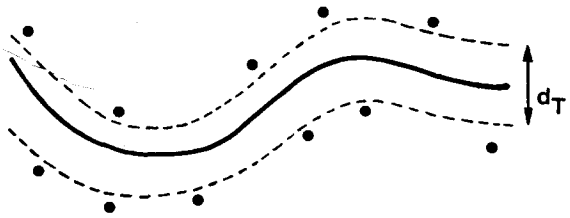

FIG. 1. Schematic representation of the pure reptation model in which the entanglements due to the neighboring chains, whose cross section is denoted by the solid circles, act to confine the chain of interest to a tube of diameter d_T.

the size of a single chain segment, $g(t) \sim t^{1/2}$ [the initial $g(t) \sim t$, predicted for very short times within the framework of the Rouse model,[9] could also be recovered in spite of the discrete character of the lattice dynamics]. We then observed a region where $g(t) \sim t^b$, which is followed by a longer time "free draining" regime, where $g(t)$ is again proportional to $t^{1/2}$. The t^b regime of $g(t)$ seems to be independent of chain length and reflects a local relaxation process, with b varying smoothly with density from the free draining value of one-half at low concentrations, i.e., below $\phi = 0.25$, to zero at a density $\phi_G = 0.92$. Thus, at very high densities, $\phi > \phi_G$, only local density fluctuations persist, thereby yielding a self-diffusion coefficient of the center-of-mass D equal to zero. Since this situation is very similar to that seen in real glassy polymers,[10,11] ϕ_G has been identified as the glass transition density.[8,12]

In the present paper, we extend our MC simulation of the dynamics of a diamond lattice, multichain system to much longer times, corresponding to the center-of-mass diffusion of the polymer coil. Hence, the dependence on chain length and concentration of the self-diffusion coefficient and the terminal relaxation time τ_R of the end-to-end vector can be investigated. The largest system under consideration consists of chains of length $n = 216$ packed at a volume fraction $\phi = 0.5$. The present simulations, described in further detail below, extend the work of Kremer[13] on diamond lattice multichain systems to cover a broader range of densities and chain lengths, and where a greater number of chains are contained per MC box. For the long chain systems packed at densities $\phi = 0.5$ and $\phi = 0.75$, we would expect, and by certain criteria, indeed do find, a substantial degree of chain entanglements, estimated to be about an order of magnitude larger than those examined previously.

The study of the dynamics of polymers in the melt has long been an active area of experimental and theoretical investigation designed to elucidate the microscopic mechanism(s) by which an entangled collection of polymers moves.[6,14,15] As is well known, a successful theory of polymer melt dynamics must be able to reproduce the following experimental results for a monodisperse melt having a degree of polymerization n:

(i) The center-of-mass self-diffusion coefficient obeys[16–25]

$$D \sim n^{-2 \pm 0.2} \tag{1}$$

for $n > n_c$, a critical value of the degree of polymerization.

(ii) The steady state, shear viscosity[14]

$$\text{if } n < n_c' \quad \eta \sim n , \tag{2a}$$

$$\text{if } n > n_c' \quad \eta \sim n^{3.4} . \tag{2b}$$

It has been observed that molecular weights required for the crossover to the large n limit are different for D and η.[16]

Since our main objective is to investigate whether the reptation model is a faithful representation of the dynamics of a system of entangled polymer chains, we include in this introductory section a brief subsection which gives an overview of the reptation model. However, before presenting an overview of reptation, we first begin with a subsection which describes the Rouse model[9,26]—a model which describes the dynamics of polymer chains in the dilute (unentangled) limit. These subsections are not intended to be substitutes for the substantial literature on these subjects, but it proves convenient to refer to them at many places in the body of this paper.

A. Dynamics of Rouse-like chains

The simplest description of the dynamics of a polymer chain is given by the Rouse model[9] which is applicable to describe the long time relaxation behavior of independent polymer chains in the absence of hydrodynamic interactions (a condition believed to hold in the melt[2,15]). The essential features of this model are: (i) the motion of the polymer chain is isotropic at all times, (ii) in the absence of excluded volume, the mean-square displacement of a bead

$$g(t) = \frac{1}{n} \sum_{i=0}^{n-1} \langle [\mathbf{r}_i(t) - \mathbf{r}_i(0)]^2 \rangle \tag{3a}$$

with $\mathbf{r}_i(t)$ the vector locating ith bead at time t and the bracket denotes the ensemble average, obeys for a chain without excluded volume

$$g(t) = 6Dt + 3D\tau_1 \sum_{k=1}^{n-1} (1 - e^{-2t/\tau_1 \sin^2(k\pi/2n)}) \times \sin^{-2}(k\pi/2n) . \tag{3b}$$

Here τ_1 is the time required to diffuse a distance equal to the effective bond length b_0 and D is the center-of-mass self-diffusion coefficient. In the limit of large n,

$$g(t) \sim t^{1/2} \quad \text{for } t < n^2\tau_1 = \tau_{\text{Rouse}} . \tag{3c}$$

τ_{Rouse} is the terminal relaxation time of the end-to-end vector, and

$$g(t) \sim t \quad \text{for } t > \tau_{\text{Rouse}} . \tag{3d}$$

(iii) At all times, the mean-square displacement of the center-of-mass,

$$g_{\text{c.m.}}(t) = \langle [\mathbf{R}_{\text{c.m.}}(t) - \mathbf{R}_{\text{c.m.}}(0)]^2 \rangle , \tag{4a}$$

with $\mathbf{R}_{\text{c.m.}}(t)$ the vector locating the center-of-mass at time t, is given by

$$g_{\text{c.m.}}(t) = 6Dt \tag{4b}$$

[note that Eq. (4b) must hold for any model of polymer motion in the limit of long times], where in the Rouse mod-

el[9,15,26]

$$D \sim n^{-1} . \tag{4c}$$

(iv) Finally,

$$\eta \sim n . \tag{5}$$

Clearly then, while the Rouse model describes the scaling behavior of D and η for low molecular weight melts [e.g., see Eq. (2a)], it does not describe their behavior in the high molecular weight limit.

B. The dynamics of reptating chains

In the "pure" reptation model (assumed to be valid for all chains in the limit of large n), lateral fluctuations of the chain are taken to be small[1–5,27,28]; the chain can only move long distances by slithering out the ends of the tube (see Fig. 1). The tube renewal time τ_{rep} is thus the time required for the end of a chain to move down its entire contour length defined at zero time and is given by

$$\tau_{\rm rep} = \tau_1 n^3 / n_e . \tag{6}$$

Since a chain moves a distance of the root-mean-square end-to-end vector in space in a time $\tau_{\rm rep}$:

$$D = D_{\rm rep} = \frac{n_e b_0^2}{\tau_1 n^2} . \tag{7}$$

In the above, n_e is the average number of monomers between entanglement points, and b_0 is the effective bond length. It follows from reptation theory[4–6] that

$$\eta \sim \tau_{\rm rep} . \tag{8}$$

Furthermore, $g(t)$ is predicted to exhibit the following behavior as a function of time. If $g(t)$ is less than the tube diameter d_T, then the chain should behave like a free Rouse chain:

$$g(t) \sim t^{1/2} \quad \text{for } t < \tau_e . \tag{9}$$

In the intermediate regime, lateral fluctuations are unimportant and the chain behaves like a one-dimensional Rouse chain confined to a Gaussian tube, which then gives

$$g(t) \sim t^{1/4} \quad \text{for } \tau_1 n_e^2 < t \leqslant \tau_1 n^2 . \tag{10}$$

($\tau_1 n^2$ is frequently called the defect diffusion time.) Furthermore, if $\tau_1 n^2 < t \leqslant \tau_1 n^3 / n_e$, the chain and the center-of-mass diffuse freely in a Gaussian tube, until the tube renewal time $\tau_{\rm rep}$[27,28]:

$$g(t) \sim t^{1/2} \quad \text{if } \tau_1 n^2 < t < \tau_{\rm rep} . \tag{11}$$

Finally, for $t > \tau_{\rm rep}$, one finds that $g(t)$ exhibits free diffusion behavior. Namely,

$$g(t) \sim t \quad \text{for } t > \tau_1 n^3 / n_e . \tag{12}$$

In a similar fashion,

$$g_{\rm c.m.}(t) \sim t \quad \text{if } t < \tau_1 n_e^2 . \tag{13}$$

Then, as indicated by simulations of chains moving in a frozen environment[13,29] and implicit in the analysis of de Gennes[2,11] the anomalous diffusion behavior

$$g_{\rm c.m.}(t) \sim t^{1/2} \quad \text{if } \tau_1 n_e^2 \leqslant t \leqslant \tau_1 n^3 / n_e \tag{14}$$

is predicted, although the Doi–Edwards theory requires for a finite tube that $g_{\rm c.m.}(t)$ be proportional to t at all times.[4]

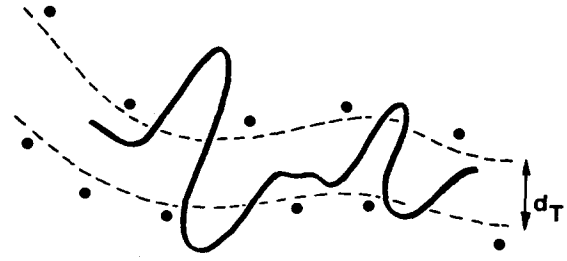

FIG. 2. Schematic representation of reptation-plus-tube-leakage model which allows for fluctuations in the primitive path length.

Finally,

$$g_{\rm c.m.}(t) \sim t \quad \text{for } t > \tau_1 n^3 / n_e . \tag{15}$$

1. Reptation-plus-tube leakage

As schematically depicted in Fig. 2, later refinements of the reptation model allowed for the possibility of tube leakage[6] or equivalently fluctuations in the primitive path length of the Doi–Edwards model.[30] In this expanded model, reptation out the tube ends remains the dominant mechanism for long distance motion. Thus, lateral fluctuations remain small, and the tube remains very well defined. Doi has invoked a tube fluctuation mechanism to rationalize the apparent 3.4 power molecular weight dependence of the viscosity (η calculated from pure reptation theory is greater than the experimentally observed η). Needs in a Monte Carlo simulation indeed found a lowering of the viscosity; but for the range of molecular weight he studied $\eta \sim n^{3.07}$.[31] Perhaps the range of primitive path lengths studied was too small; however, the further examination of these questions is beyond the scope of the present work.

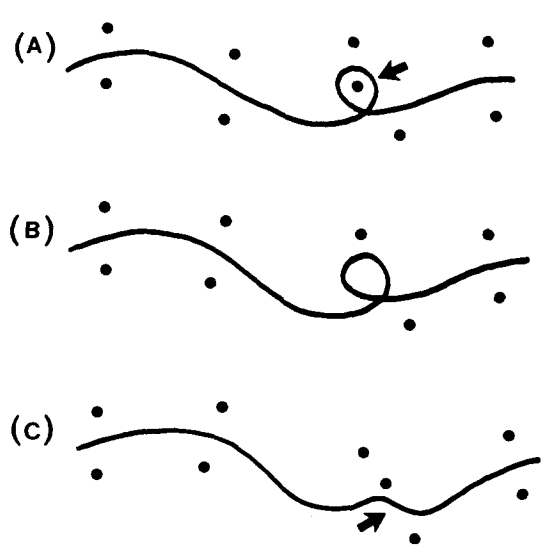

FIG. 3. Schematic representation of the reptation-plus-constraint-release model. (A) The constraint due to a neighboring chain is denoted by an arrow in Fig. 3(A). (B) It is removed in Fig. 3(B) when that chain reptates along its entire length. (C) In Fig. 3(C), some time later the constraint is replaced. This mechanism introduces new orientations in the primitive path of the black chain without requiring it to slither out the ends of the original tube.

2. Reptation-plus-constraint release

One of the possible problems with the pure reptation picture is that it is not self-consistent. To alleviate this problem, Klein,[23,33] Daoud and de Gennes,[34] and Graessley[6] introduced the constraint release or tube renewal mechanism schematically depicted in Figs. 3(A)–3(C). The constraint indicated by an arrow in Fig. 3(A) is removed when the constraining chain reptates along its length as indicated in Fig. 3(B). Then, as shown in Fig. 3(C), some time later the constraint is replaced. This introduces a new orientation into the primitive path of the chain of interest without requiring it to slither out the tube ends. Because the mechanism of tube renewal proceeds entirely by reptation of the chains forming the confining tube, lateral fluctuations of the chain within the tube remain small.

Assuming that reptation of the chain of interest and constraint release are independent mechanisms, Daoud and de Gennes[34] and Graessley[6] find for a monodisperse melt of chains (and implicit in the work of Klein[32]),

$$D = D_{\rm rep}\left(1 + \alpha_{\rm cr}\frac{n_e}{n^2}\right) \tag{16a}$$

with $D_{\rm rep}$, given by Eq. (7), and where Graessley gives[6]

$$\alpha_{\rm cr} = \frac{48}{25} z\left(\frac{12}{\pi^2}\right)^{z-1} \tag{16b}$$

with z the number of bars surrounding each cell whose linear dimensions are a primitive path length (on the order of d_T). If we take $z = 5$ (at the high end of physically plausible values[25]), then it follows from Eq. 16(b) that when $n > 4.6\, n_e$ reptation should dominate.

Equation 16(b) was derived assuming that all constraints release independently. In the nonindependent, constraint release model of Klein,[33]

$$D = D_{\rm rep}\,(1 + n_e^2/n^{3/2})\,. \tag{17}$$

Thus, pure reptation should dominate when $n > (n_e)^{4/3}$, i.e., when n is greater than a few entanglement lengths.

For additional details concerning reptation theory, we refer the reader to the literature.[1,6]

C. Objectives of the present work

The models of pure reptation, reptation-plus-tube-leakage, and reptation-plus-constraint-release present the following qualitative description of polymer melt dynamics. First, the tube is a well defined quantity; when $n > n_e$, lateral fluctuations of the chain become negligible. Second, the crossover regime from Rouse behavior where n is on the order of n_e to that where $n \gg n_e$ is dominated by the reptation mechanism. That is, lateral fluctuations of the chain are predicted to very quickly become unimportant. These are the qualitative features which form the essential basis of reptation theory, and in the context of a diamond lattice simulation, the main objective of this paper is to see if they hold. In other words, if we can find a regime in the simulation that exhibits the experimentally observed molecular weight dependence of D and τ_R on n (and we demonstrate below that such a regime does exist) then for times such that reptation theory predicts the tube is well defined, is the dominant motion of the model chains down the primitive path defined at zero time? That is, are lateral fluctuations large or small? If the lateral fluctuations are large (and we shall show this to be the case) it would, at the very least, argue for the existence of a crossover regime between pure Rouse behavior and reptation behavior that is not "reptation-like." Of course, we recognize that any finite length simulation which fails to find reptation as the dominant mechanism of long wavelength motion cannot prove that reptation does not hold in the limit of very long chain length. Nevertheless, real polymers are finite. Thus, the elucidation of the dynamics of finite length polymer chains in the diamond lattice model of a polymer melt is the focus of this paper.

The advantage of employing a lattice model of a polymer melt is that it allows us to simulate much longer polymers, at higher densities and for longer times than in the corresponding off-lattice systems.[13] The disadvantage of course is that we must demonstrate that the obtained results are physically meaningful and not lattice artifacts. For the long distance motions that form the focus of this paper, we would expect lattice effects to be unimportant. Wherever possible, we shall demonstrate the validity of the qualitative results by showing that equivalent results are found in off-lattice simulations.[29,35] However, of most crucial importance in establishing that this model system has physically realistic behavior is the demonstration that diamond lattice multichain systems exhibit the experimentally required $D \sim n^{-2\pm0.2}$ and $\tau_R \sim n^{3.4\pm0.2}$. (Unfortunately, we do not know how to extract η from a MC simulation in a *model independent* fashion.) Once having established that the long time dynamics of the real and the model systems are compatible, we shall then investigate the details of the dynamics of the model system as described above.

D. Outline of the remainder of the paper

The choice of the parameters used in the dynamics of the model system is discussed in Sec. II along with some details of the sampling procedure. The method of generation of the initial configuration of dense multichain systems and of the equilibration of the system can be found elsewhere.[8] Then in Sec. III, the results of the simulation are presented. The effect of density on the chain length dependence of the self-diffusion coefficient and the relaxation time of the end-to-end vector is examined in the context of the theoretical predictions of the Rouse and reptation models. Furthermore, the motion of an individual segment is analyzed as a function of its position along the chain contour. We then decompose the motion of the chain into components down and transverse to the original primitive path. Snapshots of the equivalent chain, where local fluctuations have been averaged out (and which is presumably close to the Edward's primitive path[36]) as a function of time are also presented. To check the ability of the analysis to demonstrate reptation, the dynamics of a single chain in a partially frozen environment is examined. Then, the relevance of the model to the real polymer systems and some limitations of the lattice approximation are discussed in Sec. IV. Finally, we summarize the major findings of the work in Sec. V.

II. MODEL AND SAMPLING PROCEDURE

The model system consists of a monodisperse collection of polymer chains confined to a tetrahedral lattice. Every chain occupies n lattice vertices, also referred to as a "beads," connected by $n-1$ "bonds." If there are N chains per MC box, subject to periodic boundary conditions, the volume fraction of the polymer is $\phi = N \cdot n/V$, where $V = L^3/8$, the number of lattice sites per MC box of edge length L. The factor of 8 results from an integer representation of the diamond lattice vertices. Thus, a single bond vector l is of length $3^{1/2}$ where l is of the form $[\pm 1, \pm 1, \pm 1]$, subject to appropriate restrictions that preserve the tetrahedral valence angles. The initial configuration of each system (N,n,L) has been carefully equilibrated,[8] and static properties have been measured to insure proper relaxation to thermal equilibrium.

A. Model of dynamics and the single chain test

A stochastic MC lattice model for polymer dynamics was introduced 25 years ago by Verdier and Stockmayer.[37] In the original version of the model, the Brownian motion of a simple cubic lattice chain was simulated by means of a random sequence of single bead jumps resulting from the permutation of two adjacent bond vectors. It has been shown that this model is equivalent to the Rouse model with $D \sim n^{-1}$ and $\tau_R \sim n^2$.[38,39] However, the introduction of excluded volume (i.e., the prohibition of the multiple occupancy of lattice sites) led to an unexpectedly strong increase of the relaxation time of the end-to-end vector, τ_R, and other relevant properties.[40] For example, $\tau_R \sim n^3$ was found instead of the theoretically expected $\tau_R \sim n^{2.2}$. Modifications of the model, by allowing the permutation of three successive bonds (two-bead jumps) does not change the n^3 dependence of τ_R.[41] The underlying explanation has been provided by Hilhorst and Deutch[42] and Boots and Deutch[43] who showed that the n^3 dependence is built into the model; the only way to create a new orientation of the middle bonds is diffusion starting from the free chain ends down the chain backbone. Introduction of two-bead, 90° crankshaft motions which create a new orientation of the interior chain bonds without diffusion from the ends, leads to relaxation behavior more consistent with the expected $\tau_R \sim n^{2.2}$ for a single "real" chain with excluded volume.[44,45] A similar, but not identical, situation exists for the case of diamond lattice polymers.[46,47] Thus, an appropriate choice of the set of elementary motions is essential to give the dynamics of real lattice chains.

The following set of elementary motions are employed in the present simulations (see also Refs. 8 and 47):

(i) three-bond jumps with an *a priori* probability $p(3b)$ resulting from the exchange of bonds l_i and l_{i+2}; the two beads are moved provided that $l_i \neq l_{i+2}$;

(ii) random reorientation of chain ends involving one (l_1 or l_{n-1}) or two bonds (l_1 and l_2, or l_{n-1} and l_{n-2}). The sum of the *a priori* probabilities of the one and two bond motions, $p(1b)$ and $p(2b)$, respectively, has been taken equal to $p(3b)$, with the relative frequency of one-bond to two-bond flips equal to 1:2;

(iii) four-bond (three-bead) motions, with *a priori* probability $p(4b)$, which create new orientations of bond vectors l_i and l_{i+3} within the chain; the necessay condition for this motion is that $l_i = -l_{i+3}$.

It has been shown that every conformational transition of a tetrahedral chain involving two or more beads can be decomposed into a succession of the above elementary motions.[48] Therefore, the only constraints on the dynamics come from the lattice and the excluded volume restrictions. The choice of the relative *a priori* frequency of attempts at three bond (and end flips) relative to four-bond moves has been shown to be irrelevant to the dynamics of long polymers (with appropriate time scaling) as long as both jump frequencies are of the same magnitude.[8,13] However, the values of the *a priori* probability of a particular elementary motion could affect the dependence of D and τ_R on n for short chain lengths. Therefore, appropriate choices are important to insure that we obtain the correct values of the scaling exponents for small n. We chose the *a priori* probability of a three-bond (four-bond) motion $p(3b)$ equal to 0.25 $[p(4b) = 0.75]$. This choice gives a good linear behavior of $\log D$ and $\log \tau_R$ vs $\log(n-1)$ for a phantom chain (nonreversing random walk) and a single real chain over the entire range of n, from $n = 12$ to $n = 216$. This is demonstrated in Fig. 4.

It should be noted that the present choice $p(3b) = 0.25$ is exactly equivalent to $p(3b) = 0.1$ of Ref. 8. This is because of the random searching for four-bond reorientations of the chain backbone employed in Ref. 8, which eliminates two thirds of the four-bond motions. The present definition is more straightforward, and four-bond reorientations are generated by a deterministic procedure, provided that the local conformation is appropriate. The assumption $p(3b) = 0.3$ in Ref. 8 [equivalent to $p(3b) = 0.5625$ using the present definition] gives the same exponent in $D \sim n^{\alpha}$ for $n \geqslant 30$. However, for shorter chains, slightly higher values of D are observed in the previously employed algorithm. Hence, the choice of the value of the ratio $p(3b)/p(4b)$ is important

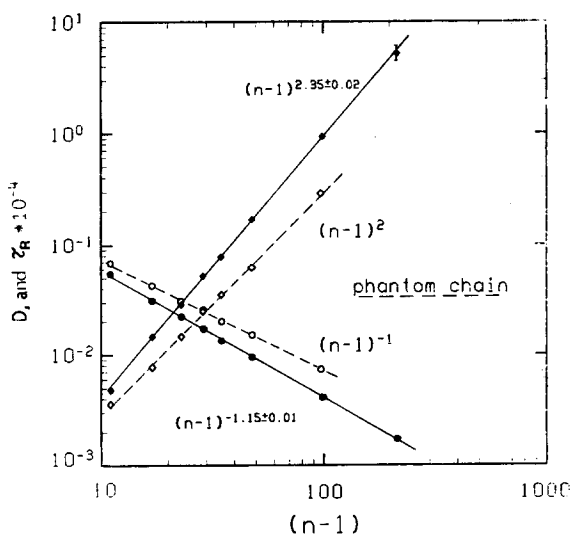

FIG. 4. Log–log plot of D and τ_R vs n for an isolated single chain in the solid (open) circles and diamonds, respectively, for a chain with (without) excluded volume.

from the point of view of computational economy (in that shorter chains could be used to study melt dynamics) and physically reflects the dynamic flexibility of the model polymers.

The algorithm works as follows:

(1) a random index is generated for the selection of a chain;

(2) a random index is generated for selection of one of the chain bonds 1,2,... $(n-1)$;

(3) the kind of elementary motion is randomly selected;

(4) if the choice is a three-bond motion, it is attempted provided that the bond index is an inner one. For an end bond, an additional random decision is required to select either a two-bond or one-bond end flip—the probability of a two-bond flip has been set to $2/3\,p(3b)$; the probability of a one-bond flip is $1/3\,p(3b)$;

(5) if the choice is a four-bond motion, the attempt is made provided the bond is an inner one.

The unit of time is the time required for $N(n-1)$ cycles, as described above, to be performed. Thus we have on average $3p(3b) + 4[1 - p(3b)]$ attempts to move every inner bond per time unit. For $p(3b) = 0.25$ this gives 3.75 attempts per bond.

B. Sampling procedure

The algorithm described in the previous subsection has been used for the simulation of the time evolution of a variety of systems defined by the number of chains per MC box, the chain length and the box size (N,n,L). The configuration of the system under consideration has been recorded at time intervals which depended on n and ϕ. In most cases, the sampling time was sufficient to obtain good statistics in the diffusion limit of the polymer chain. This means that the final mean-square-displacement of the center-of-mass of a chain was several times larger than mean-square radius-of-gyration, $\langle S^2 \rangle$. The MC box size used was always considerably larger than the mean-square end-to-end vector of the polymer coil. The effect of box size (or equivalently N at fixed ϕ) on the computed properties was checked for shorter chains (up to $n = 49$). We found that if the number of chains per MC box is greater than about 20 the computed properties are insensitive to the choice of box size. We have assumed that this conclusion remains valid in systems of longer chains containing 20 or more chains per MC box. The parameters of the sampling procedure for the most extensively studied systems are summarized in Table I. The values of the mean-square radius of gyration, and the final displacement of the center-of-mass of the polymer coil during the sampling period are also given for comparison. Some of the values of this last quantity have a lower statistical accuracy, since they were estimated from a "single" run (average over N chains). Being time averages over many pieces of the trajectory, the data used for the calculation of the autocorrelation functions are much more accurate.

C. Static properties

In Fig. 5, the expansion factor, $\alpha_S^2 = \langle S^2 \rangle / \langle S_0^2 \rangle$ is given as a function of chain length $(n-1)$ at several densities. Here, $\langle S_0^2 \rangle$ is the value of the radius of gyration for the lattice representation of an ideal, rotational isomeric states (RIS) chain.[49] For $\phi = 0.5$ and 0.75, a crossover is observed from self-avoiding random walk (SAW) chain behavior in very short chains where $\alpha_S^2 \sim n^{0.18}$ (as in the $\phi = 0$ case, for all n shown) to quasiideal behavior for long chains,[2] $\alpha_S^2 \sim n^0$. In the latter case, the excluded volume effect is screened out by interchain interactions. The limiting value of α_S^2 is close to 1.10, which has been observed in previous MC simulations.[13,50,51] The screening length n_B defined as the lowest value of n where α_S^2 lies below the $\phi = 0$ result, decreases with increasing concentration, and based on the data given in Fig. 5, can be roughly estimated as $n_B \leqslant 18$ when $\phi = 0.5$ and $n_B \leqslant 12$ when $\phi = 0.75$.

In Figs. 6 and 7, the density distribution of beads, $\rho(r_{ij})$,

TABLE I. Summary of the dense systems studied.

n	N	L	$\langle S^2 \rangle$	$g_{\text{c.m.}}(t_{\max})$[a]
		$\phi = 0.5$		
12	108	24	10.23	···
18	48	24	17.11	···
24	36	24	23.78	···
36	24	24	36.56	···
49	28	28	52.67	4372
100	40	40	111.5	1556
216	32	48	244.2	1496
		$\phi = 0.75$		
12	32	16	10.02	···
24	54	24	23.60	···
49	42	28	51.33	982.9
96	32	32	109.2	320.3

[a] $t_{\max}$ is the maximum time of sampling.

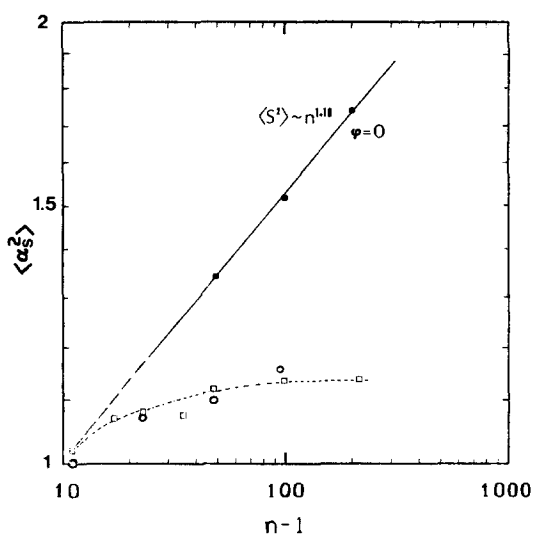

FIG. 5. Plot of the expansion factor of the radius-of-gyration $\alpha_S^2 = \langle S^2 \rangle / \langle S_0^2 \rangle$ vs log n, at $\phi = 0$ (solid circles), $\phi = 0.5$ (open squares), and $\phi = 0.75$ (open circles), respectively. $\langle S_0^2 \rangle$ is the value appropriate for an ideal, rotational isomeric state chain confined to a tetrahedral lattice (Ref. 49). Based on scaling theory we would except $\langle S^2 \rangle \sim \phi^{-1/2}$ and thus the data at $\phi = 0.5$ should be above the data at $\phi = 0.75$. However, within the error of the simulation the two cases appear to be indistinguishable.

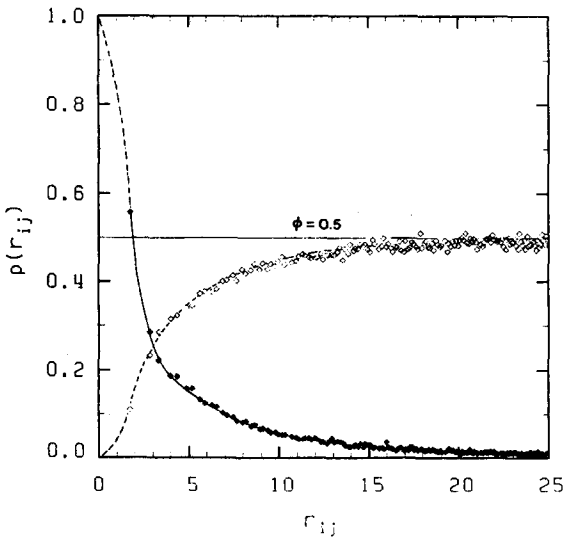

FIG. 6. Density distribution of beads, $\rho(r_{ij})$ vs the distance of separation of bead j from bead i centered at the origin, and belonging to the same chain (other chains) in the solid (open) diamonds for chains with $n = 216$ packed at $\phi = 0.50$.

belonging to the same chain (solid symbols) and to the surrounding chains (open symbols) are plotted for the case $n = 216$ at $\phi = 0.5$ and $n = 96$ at $\phi = 0.75$, respectively. Note that for the system at $\phi = 0.5$, the density of surrounding chains dominates $\rho(r_{ij})$ for distances greater than two bond lengths; while for the $\phi = 0.75$ system even in spite of chain connectivity, the second coordination sphere is mostly occupied by the segments of other chains.

An approximate estimate of the excluded volume screening length ξ can be obtained by assuming $\phi^* \cong 8N/\langle R^2_{\rm SAW}\rangle^{3/2}$ ($\langle R^2_{\rm SAW}\rangle$ is the mean-square value of the end-to-end vector of a self-avoiding walk polymer[2]; the factor of 8 is related to the diamond lattice). Then $\xi = \langle R^2_{\rm SAW}\rangle^{1/2}(\phi^*/\phi)^{3/4}$. This gives $\xi \simeq 4$ for $\phi = 0.5$ and $n = 216$, and $\xi \simeq 2.5$ for $\phi = 0.75$ and $n = 96$, consistent with the analysis of the bead distribution profiles given in Figs. 6 and 7, respectively. The above results for ξ are smaller by a factor of about 2–3 than those estimated from the dependence of $\langle S^2\rangle$ on n (see Fig. 5) when one applies the nonreversing, random walk formula[52] for the blob size, i.e., $\xi^2 = 6n_B - 4.5$. However, even using the latter values of ξ for the screening length strongly suggests that systems having $\phi = 0.5$ and greater are suitable models of highly entangled, long chain polymer systems, e.g., polymer melts or very concentrated polymer solutions.

III. RESULTS

A. Diffusion coefficients and terminal relaxation times

In order to obtain the diffusion constant we measured the center-of-mass autocorrelation function, $g_{\rm c.m.}(t)$, defined in Eq. (4a) which is then related to the self-diffusion coefficient by Eq. (4b). Both "phantom" and real single chain systems were found to exhibit behavior consistent with $g_{\rm c.m.}(t) \sim t^1$ for times greater than that required for the average displacement of the center of gravity to be only slightly larger than a single bond length. Thus the model system in the $\phi = 0$ limit behaves like a Rouse chain[9,26] [see Eq. (4b)]. In dense systems, however, there is a well defined deviation from Rouse-like results over distances such that $l^2 < g_{\rm c.m.}(t) < 2\langle S^2\rangle$ where

$$g_{\rm c.m.}(t) \sim t^a \tag{18}$$

with a only very weakly dependent on chain length and polymer concentration [actually, there is a crossover from the t^1 infinite dilution behavior of $g_{\rm c.m.}(t)$ in the range of very short chains, $n \cong 12$–24; the particular (small) value of n at the crossover is concentration dependent]. This behavior is illustrated in Figs. 8 and 9, where log–log plots of $g_{\rm c.m.}(t)$ vs t are shown for $\phi = 0.5$ and 0.75, respectively. The arrow cor-

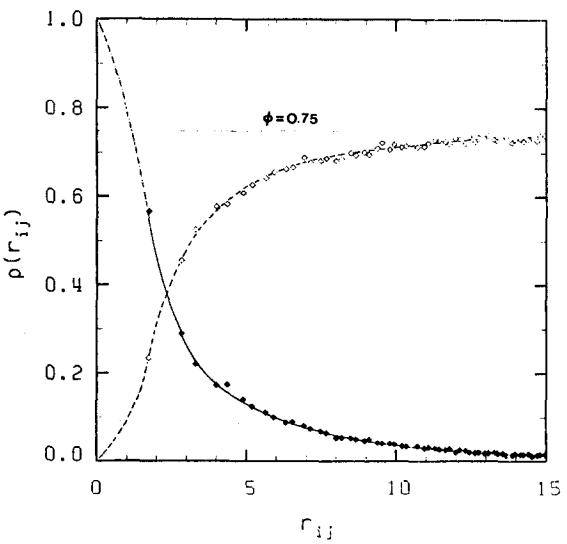

FIG. 7. Density distribution of beads, $\rho(r_{ij})$ vs the distance of separation of bead j from bead i centered at the origin, and belonging to the same chain (other chains) in the solid (open) diamonds for chains with $n = 96$ packed at $\phi = 0.75$.

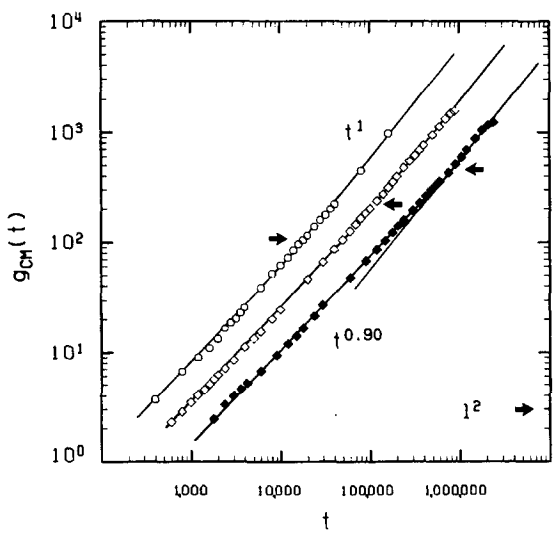

FIG. 8. Log–log plot of $g_{\rm c.m.}(t)$ vs t for chains having $n = 49$, 100, and 216 packed at $\phi = 0.50$ in the open circles, open diamonds, and solid diamonds, respectively. $g_{\rm c.m.}(t)$ is defined in Eq. 4(a). The solid arrow denotes the time at which $g_{\rm c.m.}(t) = 2\langle S^2\rangle$.

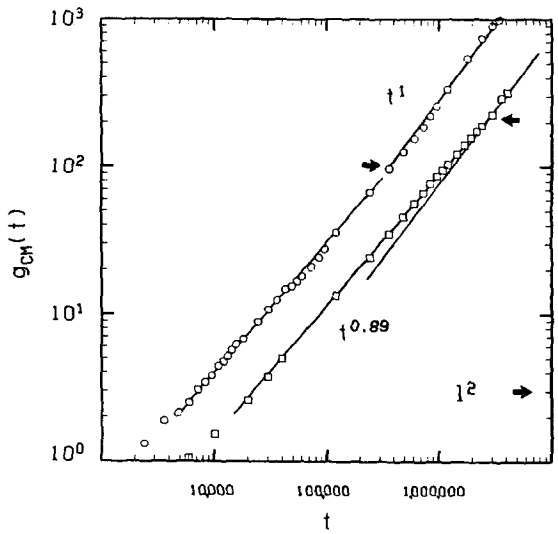

FIG. 9. Log–log plot of $g_{c.m.}(t)$ vs t for chains having $n = 49$ and 96 packed at $\phi = 0.75$ in the open circles and open diamonds, respectively. $g_{c.m.}(t)$ is defined in Eq. (4a). The solid arrow denotes the time at which $g_{c.m.}(t) = 2\langle S^2\rangle$.

responds to $g_{c.m.}(t) = 2\langle S^2\rangle$. From these plots the estimated slope is $a = 0.89$ when $\phi = 0.5$ and $n = 216$ and $a = 0.90$ when $\phi = 0.75$ and $n = 96$. Hence, there is a small, but apparently real, deviation from the simple Rouse chain t^1 behavior. Moreover, the dependence of $g_{c.m.}(t)$ on time is also inconsistent with that predicted from the reptation model [see Eqs. (13)–(15)]. Interestingly, $2\langle S^2\rangle$ is precisely the distance over which, $g_{red}(t)$, defined as

$$g_{red}(t) = \frac{1}{n}\sum_{i=1}^{n}\langle\{[\mathbf{r}_i(t) - \mathbf{R}_{c.m.}(t)] - [\mathbf{r}_i(0) - \mathbf{R}_{c.m.}(0)]\}^2\rangle \quad (19)$$

reaches its plateau value for a Rouse-like chain; i.e., it is the displacement distance corresponding to the time beyond which the internal modes of a Rouse chain have relaxed to their equilibrium values. The deviation in $g_{c.m.}(t)$ from linear behavior appears to reflect a coupling of the center-of-mass motion of a given chain to the internal modes of the test chain and the other chains. This provides the first indication that there is a cooperative aspect to the motion in this model of a polymer melt that is neither accounted for by a Rouse nor a reptation description of the dynamics. [We point out that a similar t^a behavior has been observed by Bishop *et al.* in an off-lattice simulation[35]; i.e., the behavior of $g_{c.m.}(t)$ vs t embodied in Eq. (18), is not an artifact of the lattice.] Furthermore, a similar behavior in $g_{c.m.}(t)$ vs t is evident in Kremer's simulation (see Fig. 7 of Ref. 13) for a chain of $n = 200$ at $\phi = 0.344$.

The deviation in $g_{c.m.}(t)$ from a linear dependence on time at distances below $2\langle S^2\rangle$ requires us to employ the following procedure to obtain a correct estimate of the diffusion coefficient. First, we have found for all the systems (N,n,ϕ) studied here that the crossover from the t^a to the t^1 regime is indeed located at $g_{c.m.}(t) \simeq 2\langle S^2\rangle$. Then, we fit the data for $g_{c.m.}(t) \geqslant 2\langle S^2\rangle$ to the linear function

$$g_{c.m.}(t) = 6Dt + c\,. \quad (20)$$

The constant c usually has a small positive value related to the initial t^a regime and is related to the more rapid apparent diffusion at distances less than $\sqrt{2}\langle S^2\rangle^{1/2}$. A similar analysis has been employed by Evans and Edwards[27] to extract D for the reptation dynamics of a primitive path. The values of the self-diffusion coefficient for the various systems studied are compiled in column three of Table II.

The second property extracted from the MC data is the longest relaxation time τ_R calculated from the decay of the end-to-end vector (R) correlation function,

$$g_R(t) = \langle \mathbf{R}(t)\cdot\mathbf{R}(0)\rangle/\langle R^2\rangle\,. \quad (21)$$

In spite of some deviations in our system from pure Rouse dynamics, we will show below that the set of Rouse normal coordinates is applicable for the description of the polymer relaxation in our model system. Therefore we would expect that

$$g_R(t) \sim \exp(-t/\tau_R)\,. \quad (22)$$

In Fig. 10, we present a semilog plot of $g_R(t)$ vs t for the $n = 216, \phi = 0.5$ and $n = 96, \phi = 0.75$ systems in the curves denoted by filled in and open diamonds, respectively. As clearly shown in Fig. 10, after a short initial period of very fast relaxation the correlation function indeed decays exponentially. The rapid initial decay seems mostly to be related to the higher mobility of chain ends in dense systems at short times (which will be discussed later in more detail), and reflects the contribution of shorter relaxation times. Since

TABLE II. Diffusion coefficient D and τ_R.[a]

n	ϕ	D	τ_R
12	0	$5.46\cdot10^{-2}$	$0.48\cdot10^{2}$
18	0	$3.10\cdot10^{-2}$	$1.45\cdot10^{2}$
24	0	$2.22\cdot10^{-2}$	$2.85\cdot10^{2}$
30	0	$1.74\cdot10^{-2}$	$5.22\cdot10^{2}$
36	0	$1.33\cdot10^{-2}$	$7.80\cdot10^{2}$
49	0	$0.95\cdot10^{-2}$	$1.68\cdot10^{3}$
100	0	$4.15\cdot10^{-3}$	$9.3\cdot10^{3}$
216	0	$1.73\cdot10^{-3}$	$5.2\cdot10^{4}$
24	0.125	$1.45\cdot10^{-2}$	$3.76\cdot10^{2}$
49	0.125	$0.63\cdot10^{-2}$	$2.52\cdot10^{3}$
12	0.25	$2.56\cdot10^{-2}$	$0.69\cdot10^{2}$
18	0.25	$1.38\cdot10^{-2}$	$2.36\cdot10^{2}$
24	0.25	$0.90\cdot10^{-2}$	$4.44\cdot10^{2}$
36	0.25	$5.03\cdot10^{-3}$	$1.46\cdot10^{3}$
49	0.25	$3.43\cdot10^{-3}$	$3.02\cdot10^{3}$
24	0.375	$5.24\cdot10^{-3}$	$8.35\cdot10^{2}$
12	0.5	$9.74\cdot10^{-3}$	$1.85\cdot10^{2}$
18	0.5	$4.56\cdot10^{-3}$	$6.20\cdot10^{2}$
24	0.5	$2.76\cdot10^{-3}$	$1.30\cdot10^{3}$
36	0.5	$1.49\cdot10^{-3}$	$4.75\cdot10^{3}$
49	0.5	$0.94\cdot10^{-3}$	$1.14\cdot10^{4}$
100	0.5	$3.09\cdot10^{-4}$	$6.9\cdot10^{4}$
216	0.5	$0.86\cdot10^{-4}$	$5.2\cdot10^{5}$
24	0.625	$1.05\cdot10^{-3}$	$3.80\cdot10^{3}$
12	0.75	$1.09\cdot10^{-3}$	$1.17\cdot10^{3}$
24	0.75	$2.36\cdot10^{-4}$	$1.15\cdot10^{4}$
49	0.75	$5.08\cdot10^{-5}$	$1.75\cdot10^{5}$
96	0.75	$1.13\cdot10^{-5}$	$1.52\cdot10^{6}$

[a] The numerical values of D and τ_R are expressed in time units defined at the end of Sec. II A. D is also related to the model units of length, where $l^2 = 3$. However, the scaling of τ_R and D with chain length and concentration is independent of our arbitrary choice of units.

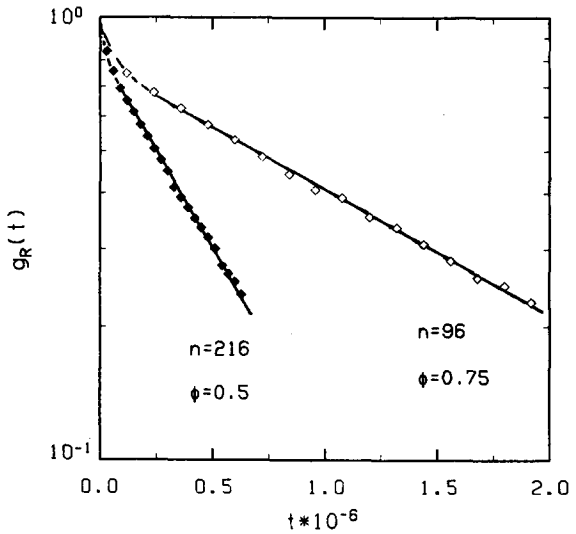

FIG. 10. Semilog plot of $g_R(t)$ vs $10^{-6}\,t$ for chains having $n = 216$ and $\phi = 0.5$ ($n = 96$ and $\phi = 0.75$) in the solid (open) diamonds. $g_R(t)$ is defined in Eq. (21).

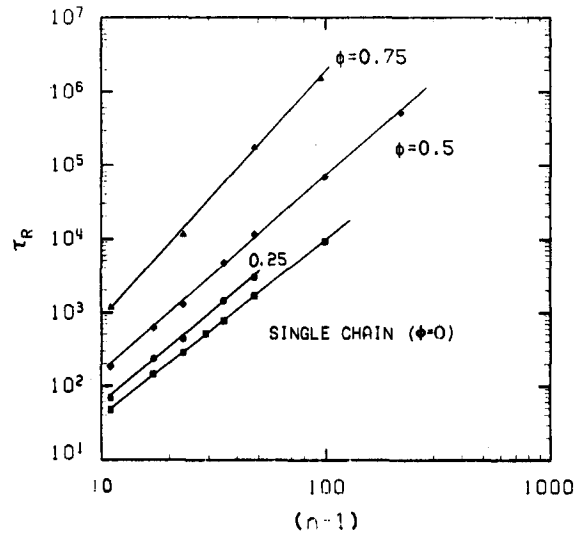

FIG. 12. Log–log plot of τ_R vs $(n-1)$ at various densities, with τ_R the terminal relaxation time of the end-to-end vector.

the MC data for the very small values of $g_R(t)$ exhibit large relative scatter, for obvious reasons, we have chosen a well defined window $0.75 > g_R(t) > 0.25$ for the estimation of τ_R. The values of the longest relaxation time are listed in column four of Table II.

1. Chain length and concentration scaling of D and τ_R

As shown in Fig. 11, the self-diffusion coefficient D scales for all densities studied as

$$D \sim (n-1)^{-\alpha}. \tag{23}$$

Equation (23) was found to hold over the entire range of n studied. The exponent α is concentration dependent and changes from $\alpha = 1.15$ at zero concentration (the case of a single chain with excluded volume) to $\alpha = 2.06$ at a density $\phi = 0.75$. As shown in Fig. 12, similar scaling behavior is observed for the longest relaxation time τ_R, as a function of chain length where

$$\tau_R \sim (n-1)^{\beta}. \tag{24}$$

At the highest concentration examined, $\phi = 0.75$, the value of the exponent approaches $\beta = 3.36$. Thus, the $\phi = 0.75$ system exhibits the experimentally observed molecular weight dependence of both D and τ_R.[2,6,15] We expect even higher values of β at higher volume fractions of polymer, which are below the glass transition density, ϕ_g. However, we have not undertaken simulations of the long time dynamics of systems whose densities exceed $\phi = 0.75$, which, due to the very rapid increase in computational time required, are beyond our capabilities. The values of α and β obtained from numerical fit of the scaling relations of Eqs. (23) and (24) at various densities to the data shown in Figs. 11 and 12 are listed in Table III.

Note that β at zero concentration is somewhat larger than the value of 2.2 predicted from some theoretical considerations.[54] A similar effect has been observed in other MC lattice dynamic studies such as those of Kovac *et al.*[54,55] Furthermore, the diffusion coefficient D at zero density exhibits a stronger dependence on chain length than the theoretically

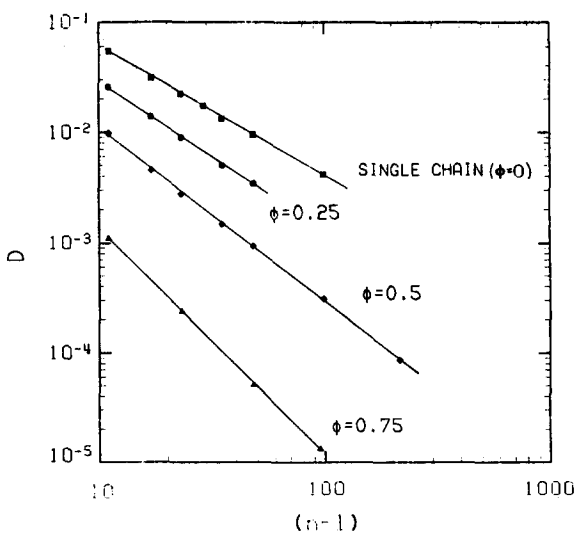

FIG. 11. Log–log plot at various densities of D vs $(n-1)$, with D the center-of-mass self-diffusion coefficient.

TABLE III. Chain length dependence of the self-diffusion coefficient, $D \sim (n-1)^{-\alpha}$, and relaxation time, $\tau_R \sim (n-1)^{\beta}$, at various concentrations.

ϕ	α	β
Single chain	1.154 ($\pm$0.010)[a]	2.349 ($\pm$0.018)[a]
0.25	1.372 ($\pm$0.021)[a]	2.563 ($\pm$0.061)[a]
0.50	1.567 ($\pm$0.017)[a]	2.677 ($\pm$0.035)[a]
0.75	2.055 ($\pm$0.016)[a]	3.364 ($\pm$0.082)[a]
0.92	2.4_2[b]	3.6_2[b]

[a] Standard deviation of the slope obtained from a linear least square fit of the log–log plot in Figs. 11 and 12, respectively.

[b] Extrapolated to the glass transition density according to the factorization approach [Eqs. (25)–(29)].

expected $D \sim n^{-1}$.[9,26] However, the product, $D\tau_R$, at $\phi = 0$ scales with an exponent which is in reasonable agreement with the expected $n^{1.2}$. Moreover, *this scaling relation between D and τ_R also holds at all higher densities*. We cannot be sure that this is not an artifact related to a coincidence of statistical uncertainties in the estimation of α and β (which is about 0.05 for each exponent at high densities). Another reason for the above caution is the slight decline in τ_R for the longest chain under consideration ($n = 216$ at $\phi = 0.5$) from the common scaling curve shown in Fig. 12. Hence, we cannot exclude the possibility that $D\tau_R \sim n$ could be recovered for much longer chains than those studied here. We point out that in a cubic lattice simulation, Crabb and Kovac's data on relatively short chains indicate that $D\tau_R \sim n^{1.1}$.[55]

As has been shown in previous work on similar model systems, the self-diffusion coefficient should approach zero at some critical density ϕ_G.[8,12] Therefore, we attempted to subtract out the effect of local friction on chain dynamics. Using a similar approach to that used by Kranbuehl and Verdier[56] and independently by Yu and co-workers,[21,57] who followed a suggestion of Schaefer,[58] we can formally write

$$D = K_D \zeta^{-1}(\phi) f_D(\phi,n) \tag{25}$$

and

$$\tau_R = K_\tau \zeta(\phi) f_\tau(\phi,n) . \tag{26}$$

We shall assume a standard free volume dependence of the monomeric friction coefficient, ζ[59]:

$$\zeta \sim \exp[-\gamma\phi/(\phi - \phi_G)] . \tag{27}$$

γ is a factor (< 1) that allows for possible overlap of free volume between segments. $\phi_G = 0.92$ was found in previous work.[8,12]

We also assumed the following forms for f_D and f_τ:

$$f_D = (n-1)^{-\alpha_0 - \lambda\phi^d} , \tag{28}$$

$$f_\tau = (n-1)^{\beta_0 + \lambda\phi^d} , \tag{29}$$

where α_0 and β_0 are the exponents from the single chain dynamics simulation at $\phi = 0$ (1.15 and 2.35, respectively). Hence, the adjustable parameters are K_D, K_τ, γ, λ, and d. Limiting ourselves to the data for $\phi \geqslant 0.25$ and $n \geqslant 49$, we are able to simultaneously fit the diffusion coefficient and relaxation time dependence on both the chain length and concentration yielding $K_D = 0.479$, $K_\tau = 0.200$, $\gamma = +0.217$, $\lambda = 1.716$, and $d = 2.125$. The fit to the diffusion data alone gives $K_D = 0.603$, $\gamma = 0.349$, $\lambda = 1.425$, and $d = 1.754$. Hence, we can extract the limiting values of the chain length dependence of D and τ_R at a density just below the glass transition density by setting $\phi = \phi_G$ in Eqs. (28) and (29) giving in the limit that $\phi \to \phi_g$:

$$D \sim (n-1)^{-2.39(2.59)} , \tag{30}$$

$$\tau_R \sim (n-1)^{3.59(3.78)} \tag{31}$$

(the values in parentheses come from using the set of parameters obtained from fitting the diffusion data only). Thus, the model exhibits a chain length dependence of the dynamic properties (D,τ_R) in reasonable agreement with experiment over a wide range of concentration. We also note that the data of Crabb and Kovac[55] are fit equally well by the above functional form. Finally, the concentration dependence of D and τ_R diverges exponentially in the vicinity of the glass density due to a local frictional effect which seems to be in agreement with recent experimental results.[21,57]

The ability of Eqs. (25)–(29) to fit the simulation data suggests (at least for the model system examined here) that the glass transition is due to the freezing out of elemental local motions which leads to the freezing out of global motions since both α and β remain finite at the glass transition density. The concentration dependence of D and τ_R further suggests that one might identify ϕ_G with the glass transition temperature T_g. If so, since the molecular weight dependence of D and τ_R increases with increasing density, which is perhaps analogous to decreasing temperature, there may perhaps be a temperature dependence of α and β as one approaches the glass transition temperature of a melt. Therefore, the possibility of anomalous molecular weight dependencies of D and τ_R should be explored.[21] However, we hasten to point out that the mapping of ϕ to the density of real systems is unknown and that the assumption of a correspondence of $\phi - \phi_G$ to $T - T_g$ may not hold. Moreover, the numerical values we obtain for α and β at the glass transition density may be model dependent. Thus, we view this prediction as being very qualitative at best.

B. Average motion of monomers

The average motion of the n monomers is described by the autocorrelation function $g(t)$ defined in Eq. (3a) or the similar function with the center-of-mass motion subtracted out $g_{\rm red}(t)$ defined in Eq. (19). In our simulations, contrary to the reptation predictions [see Eqs. (9)–(12)], we have never found a middle time regime where $g(t) \sim t^{1/4}$, which is associated with the reptation of the chain down the tube. The initial plateau regime reported in Ref. 8 is not relevant to the reptation model and reflects the constrained motion at very

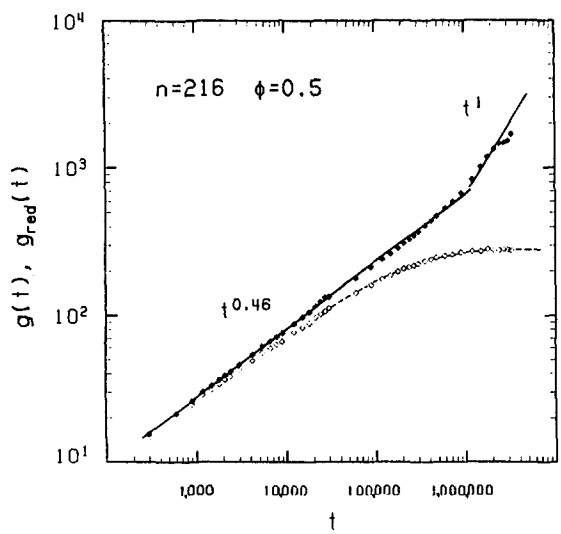

FIG. 13. Log–log plot of $g(t)$ and $g_{\rm red}(t)$ vs t, in the solid and open diamonds, respectively, calculated for the 74 middle beads of the $n = 216$ and $\phi = 0.5$ system. $g(t)$ and $g_{\rm red}(t)$ are defined in Eqs. (3a) and (19), respectively.

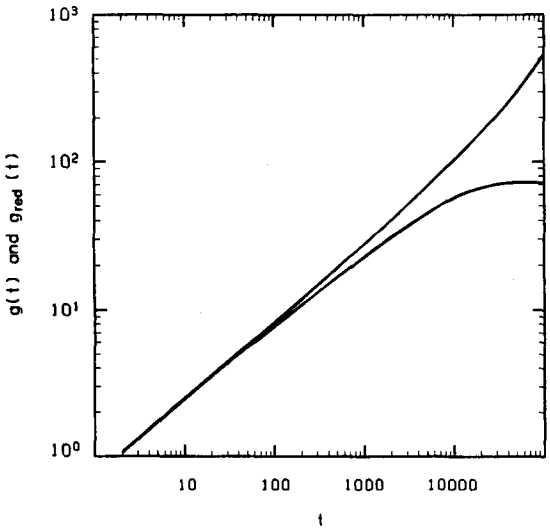

FIG. 14. Log–log plot of $g(t)$ and $g_{\rm red}(t)$ vs t in the upper and lower curves, respectively, for a Rouse chain at $n = 216$ and calculated employing Eq. (3b) for $g(t)$ and using $g(t) - 6Dt = g_{\rm red}(t)$.

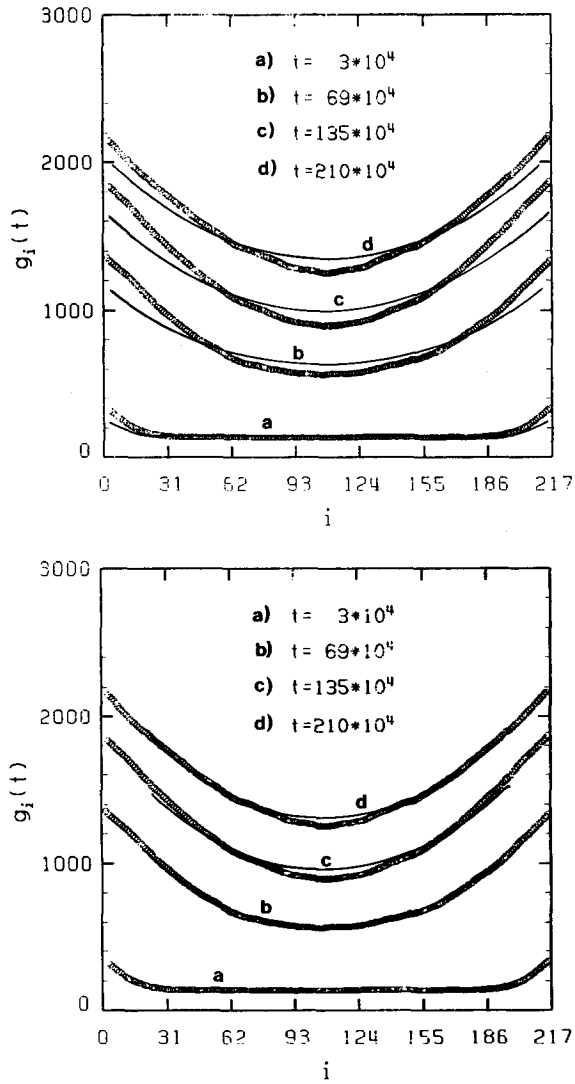

FIG. 15. Plot of $g_i(t)$ vs i, at times indicated in the figure. (A) (upper figure) For $n = 216$ chains in a melt packed at $\phi = 0.5$ in the open circles, and calculated via Eqs. (33a) and (33b) assuming that the Rouse eigenvectors form a good basis set in the solid lines. See the text for additional details. (B) (lower figure) Plot of $g_i(t)$ vs i, at times indicated in the figure, for $n = 216$ chains in a melt packed at $\phi = 0.5$ [a chain with $n = 176$ assuming Eqs. (33a) and (33b) are valid] in the open circles (solid lines). See the text for further details.

short distances of conformational defects (or free volume clusters) in a direction on the average perpendicular to the chain axis. Figure 13 presents representative log–log plots of $g(t)$ and $g_{\rm red}(t)$ averaged over the 74 middle beads vs t in the curves marked by the solid and open diamonds, respectively, for the system with $n = 216$, $\phi = 0.5$ (chains at $\phi = 0.75$ display identical behavior). The behavior of these quantities is qualitatively consistent with the prediction from the Rouse model. The small deviation from the $t^{1/2}$ dependence of $g(t)$ predicted by Rouse dynamics is just slightly beyond the statistical uncertainty of the simulation. However, it should be noted that an isolated chain with $n = 216$ obeying Rouse dynamics both with and without excluded volume exhibits a far broader crossover regime from the $t^{1/2}$ to t behavior than seen here for the chain in a melt with $\phi = 0.5$. This is graphically illustrated in Fig. 14 where we present log–log plots of the Rouse predictions for $g(t)$ and $g_{\rm red}(t)$ vs t obtained employing Eq. (3b) in the upper and lower curves, respectively.

The sharpness of the transition from the $t^{0.46}$ to t^{1} power law behavior in the melt is clearly the result of the presence of the other chains and is due to the slowing down of the internal relaxation processes that effectively results in an $n = 216$ chain being closer to the asymptotic large n limit of $g(t)$, if the dynamics can be described by a modified Rouse model. However, we point out that the presence of a one or one-half power in the exponent of $g(t)$ does not necessarily imply that Rouse dynamics holds. For example, a reptating chain when $t > \tau_1 n^2$ undergoes free diffusion within a tube and yet exhibits a $t^{1/2}$ power law dependence in $g(t)$.[2,27]

C. Profiles of single bead autocorrelation functions

We next turn to an examination of the finer details of the motion and analyze the single bead autocorrelation function $g_i(t)$ defined as

$$g_i(t) = \langle [\mathbf{r}_i(t) - \mathbf{r}_i(0)]^2 \rangle \tag{32}$$

as a function of position i along the chain. In the curves formed from the open circles in Fig. 15(A), we present a representative plot, at various times indicated in the figure, of $g_i(t)$ vs i obtained from the simulation for the system containing $n = 216$ chains packed at $\phi = 0.5$.

Using a Rouse-like formulation where we assume the Rouse eigenfunctions are a good basis set, but do not necessarily employ the Rouse eigenvalues, we can write

$$g_i(t) = \langle [\mathbf{r}_i(t) - \mathbf{r}_i(0)]^2 \rangle$$
$$= 6Dt + \frac{\langle R^2 \rangle}{n^2} \sum_{k=1}^{n-1} \cos^2[(2j+1)k\pi/2n] \times \sin^{-2}\left(\frac{k\pi}{2n}\right) \left\{1 - \exp\left[\frac{-12n^2Dt}{\langle R^2 \rangle} \sin^2 \frac{k\pi}{2n}\right]\right\}, \tag{33a}$$

where $\langle R^2 \rangle$ is the mean-square value of the end-to-end vector in the melt [which is approximately equal to 6.6 $(n-1)$ in the case of diamond lattice polymers[13,50,51]]. The only adjustable parameter in Eq. (33a) is $D(t)$, the apparent self-diffusion coefficient of the center-of-mass, which is extracted from

$$D(t) = g_{\text{c.m.}}(t)/6t, \tag{33b}$$

$D(t)$ obtained from Eq. (33b) differs at most by about 50% from its value at infinite time and monotonically decreases with increasing time. The resulting $g_i(t)$ vs i profiles obtained from Eqs. (33a) and (33b) are shown as the solid curves of Fig. 15(A) and are found to fit the profiles fairly well. However, at all times there seems to be a noticeable deviation for the end segments in that Eq. (33a) *underestimates* the mobility of the chain ends in comparison with the middle part of the chain. For longer times the deviation of $g_i(t)$ from the theoretical Rouse curves increases, with the chain ends exhibiting more and more excess mobility. This is the same trend observed in the analysis of the motion of the center-of-mass up to the time when $g_{\text{c.m.}}(t) \cong 2\langle S^2 \rangle$, where $g_{\text{c.m.}}(t) \sim t^a$ with $a < 1$ crosses over into a $g_{\text{c.m.}}(t) \sim t$ regime. We should further point out that if $D(t)$ is extracted from the profiles of $g_i(t)$, the value of $D(t)$ is essentially the same as that obtained from Eq. (33b). The higher mobility of the chain ends is probably partially due to the extra free volume at the chain ends[60,61] and also to the smaller degree of cooperativity of the motion at the chain ends due to a smaller effect of entanglements.

As shown in Fig. 15(B), at longer times the simulated $g_i(t)$ vs i (open circles) can be reproduced rather well by the theoretical expression, Eqs. (33a) and (33b) (solid lines) if only the middle of the chain composed of 176 beads (20 beads on each end of the $n = 216$ chain are omitted) is considered, using a value of $\langle R^2 \rangle$ which is correct for the chain of $n = 176$ beads and $D(t)$ extracted from Eq. (33b). In some sense, the motion of the chain behaves similarly to that of a modified Rouse chain having a larger $D(t)$, with additional corrections resulting from the significantly lower effective friction constant for the end segments.

D. Mechanism of long distance motion

Even though the single bead autocorrelation function is consistent with a modified Rouse model, the deviation of the center-of-mass motion from the t^1 power law at distances less than $\sqrt{2}\langle S^2 \rangle^{1/2}$, still remains unexplained. The enhanced apparent $D(t)$ in the t^a regime suggests that there is some cooperativity involving the coupling of the center-of-mass motion with that of the individual beads. Moreover, at $n = 216$ the narrow crossover from $t^{0.46}$ power law dependence in $g(t)$ to t^1 behavior is not accounted for in the Rouse model even with the eigenvalues modified as in Eqs. (33a) and (33b). Thus, up to now, while we have to some extent demonstrated that the dynamics of our model melt appears to be closer to a Rouse model with its assumption of isotropic motion than to a reptation model with its assumption of anisotropic motion, we have not in fact answered the crucial question that is the crux of this paper and is the essence of the current debate about the validity of the reptation model. That is, what is the character of the motion of the polymer on a distance scale large in comparison with the length of a single bond, but smaller than the coil size? Is the direction of the motion longitudinal, consistent with the reptation picture? Is there no directional preference? Or is the dominant motion transverse to the local chain axis?

1. Construction of the equivalent path

In order to directly examine the character of the long distance motion, the motion of the blobs (or segments of the primitive path[4,36]) is analyzed. First, the original model chains are replaced by equivalent paths composed of n overlapping blobs, the ith one of which such that $n_B/2 < i < n - n_B/2$ is

$$\mathbf{r}_i^*(t) = \frac{1}{(n_B+1)} \sum_{j=i-n_B/2}^{i+n_B/2} \mathbf{r}_j(t) \tag{34}$$

and for $i < n_B/2$ $(i > n - n_B/2)$, the average is over the $n_B/2 + i(n_B/2 + n - i)$ beads centered at bead i. Averaging the chain over $n_B + 1$ beads gives a smooth random curve which eliminates the small scale, local fluctuations that are irrelevant to the long distance motions and which should be very close to the primitive path of the reptation model if n_B is close to the entanglement length. If the polymer moves down the tube formed by the topological constraints imposed by the other chains, there should be substantial memory of the primitive path "conformation," at least for the middle part of the chain. Thus, the following procedure has been applied in order to extract the longitudinal and transverse components of the chain motion. As schematically depicted Fig. 16, we first computed the longitudinal displacement down the original primitive path defined by $\{\mathbf{r}_i^*\}$ at the time t_0 by projecting $\mathbf{r}_i^*(t_0 + \Delta t)$ onto the original path. If the projection of $\mathbf{r}_i^*(t_0 + \Delta t)$ is onto blob j in the original path, then the displacement of blob i down the original primitive path is

$$\Delta s = l_b |i - j|, \tag{35}$$

where l_b is the average distance between the centers of two neighboring blobs.

Thus, the mean-square longitudinal displacement down

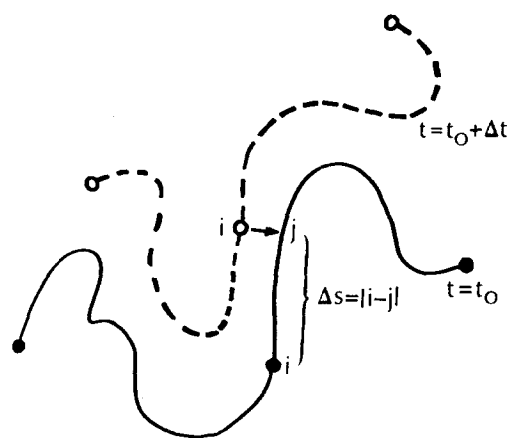

FIG. 16. Schematic representation of the primitive path at $t = t_0$ in the solid line and at $t = t_0 + \Delta t$ in the dashed line used to compute the mean-square displacement of the chain down, $g_{\parallel}(t)$, and transverse to, $g_{\perp}(t)$, the original primitive path defined at $t = t_0$.

the original primitive path, which represents the reptation component of the motion, is

$$g_{\parallel}(\Delta t) = l_b^2 \langle |i-j|^2 \rangle . \quad (36)$$

The remaining, transverse component of the motion is computed from

$$g_{\perp}(\Delta t) = \langle [\mathbf{r}_j^*(t_0) - \mathbf{r}_i^*(t_0 + \Delta t)]^2 \rangle . \quad (37)$$

In Eqs. (36) and (37), the average is over all beads in the middle third of the chain.

Observe that for a reptating chain, $g_{\perp}(t)$ has a maximum value $2/3d_T$ for times less than the tube renewal time. Thus, for that range of t, $g_{\perp}(t)/g_{\parallel}(t)$ should be very close to zero for those segments near the middle of a reptating chain.

In the context of reptation theory, the number of entanglements per chain is of crucial importance in determining whether or not pure reptation should dominate the behavior of $g_{\parallel}(t)$ and $g_{\perp}(t)$.[1,6,32–34,62] We present in Table IV a summary of the number of entanglements per chain estimated by various criteria for the $n = 216$ chains at $\phi = 0.5$ and the $n = 96$ chains at $\phi = 0.75$. If any of the measurements of the number of entanglements presented in Table IV are appropriate to describe the number of entanglements, then both by the criterion of Graessley,[6] $n/n_B > 5$, and by the criterion of Klein,[33] $n > (n_e)^{4/3}$ (which equals 47 if $n_B \simeq n_e$ where we take $n_B = 18$ for the $\phi = 0.5$ case and equals 27 for the $\phi = 0.75$ case with $n_B = 12$). Therefore, we would clearly expect to see reptation as the dominant motion.[34]

In Fig. 17, we plot $g_{\perp}(t)/g_{\parallel}(t)$ vs t for the case of a melt of chains at $n = 216$, $\phi = 0.5$ (with a corresponding $10^{-4}\,t$ time scale) and $n = 96$, $\phi = 0.75$ (with a corresponding $10^{-5}\,t$ time scale) in the open diamonds and circles, respectively. We set $n_B = 18$, a physically reasonable value (see Table IV). (The results in fact are insensitive to the choice of n_B provided that n_B exceeds some very small value.) The value of l_b^2 obtained from the simulation is 0.28, and is essentially density independent. The terminal relaxation time of the end-to-end vector for the $n = 216$, $\phi = 0.5$ case is

TABLE IV. Summary of various estimates of the number of entanglements per chain.

Method	$\phi = 0.5$, $n = 216$		$\phi = 0.75$, $n = 96$	
	n_b	n/n_b	n_B	n/n_B
Screening length of excluded volume[a]	18	12	12	8
Segment–segment density distribution function[b]	3	72	2	48
Pulling all the chain ends to count the number of knots[c]	···	10–15	···	···
Dynamics of a single chain in partially frozen environment[d]	5–11	20–43	···	···

[a] Obtained from Fig. 5 where we plot $\langle S^2 \rangle / \langle S^2 \rangle_0$ vs n. See Sec. II C.
[b] Obtained from Figs. 6 and 7 for $\phi = 0.5$ and 0.75, respectively, corresponding to the n_Bth nearest neighbor on the lattice where $\rho(r_{ij})$ of beads on other chains first exceeds $\rho(r_{ij})$ due to beads in the same chain as the bead at the origin.
[c] See Appendix A.
[d] Estimated from Fig. 21, the log–log plot of $g(t)$ vs t and obtained via the nonreversing random walk formula for n_B (Ref. 52).

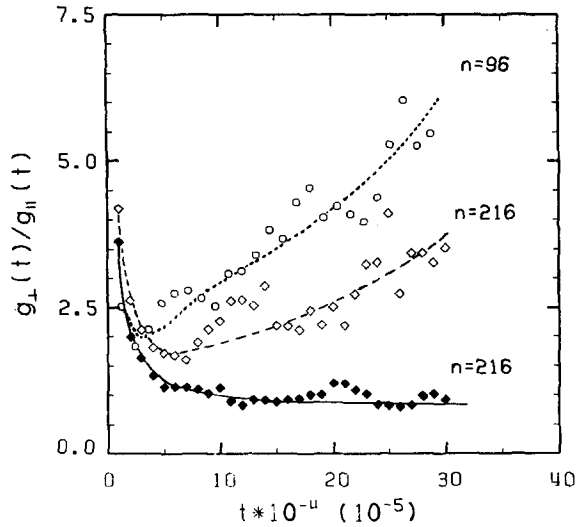

FIG. 17. Plot of $g_{\perp}(t)/g_{\parallel}(t)$ vs 10^{-4} $(10^{-5})t$ for a melt of chains with $n = 216$ and $\phi = 0.5$ ($n = 96$ and $\phi = 0.75$) in the open diamonds (circle). The solid diamonds represent $g_{\perp}(t)/g_{\parallel}(t)$ vs $10^{-4}t$ for a single chain of $n = 216$ in a partially frozen matrix of other chains pinned every 18 beads and packed at an overall density $\phi = 0.5$.

5.2×10^5, and for the $n = 96$, $\phi = 0.75$ case, is 1.52×10^6. The deviation in $g_{\perp}(t)/g_{\parallel}(t)$ from the isotropic value of 2 at shorter times ($t < 5$ in the scaled units of the graph) is due to the transverse character of the very local motions previously discussed in detail.[8] At times appreciably less than free diffusion or even the terminal relaxation time of the end-to-end vector, $g_{\perp}(t)/g_{\parallel}(t)$ is seen to *grow* monotonically with increasing time. (Similar behavior would be evidenced by a Rouse chain.) This indicates that *reptation can only comprise a small component of the motion in these model systems.* In fact, for the system at $\phi = 0.75$ which displays the $D \sim n^{-2.1}$ and $\tau_R \sim n^{3.4}$ behavior of the physical system, the memory of the original path is less (of course we must correct for the differences in molecular weight) than the system at the lower density, $\phi = 0.5$ having weaker molecular weight dependencies of D and τ_R. Nevertheless, the qualitative behavior seen in these systems as a function of ϕ indicates a smooth crossover in the D and τ_R dependence on molecular weight, with no abrupt change in behavior evident.

For convenience of the reader in Figs. 18(A) and 19(A), we present a log–log plot of $g(t)$ vs t where the arrows with corresponding letters (B)–(D) denote the time difference Δt between snapshots showing typical superimposed projections of the primitive path of a given chain with $\Delta t = 10^4$, 3×10^4, and 5×10^4 in Figs. 18(B)–18(D) and $\Delta t = 1.2\times10^5$, 3.6×10^5, and 7.2×10^5 in Figs. 19(B)–19(D), respectively. For all cases in Fig. 18 (19) $n = 216$ (96) and $\phi = 0.5$ (0.75). To differentiate between the two ends, one of the ends is labeled by a triangle. The transverse fluctuations as well as the fluctuations in the length of the primitive path are so large that the polymer moves essentially like a single chain in a dilute system; however, the time scale, and the character of the local motion, are quite different. It should be emphasized that the longest time snapshot depicted in Figs. 18 and 19 is about 1/5 to 1/10 of the time

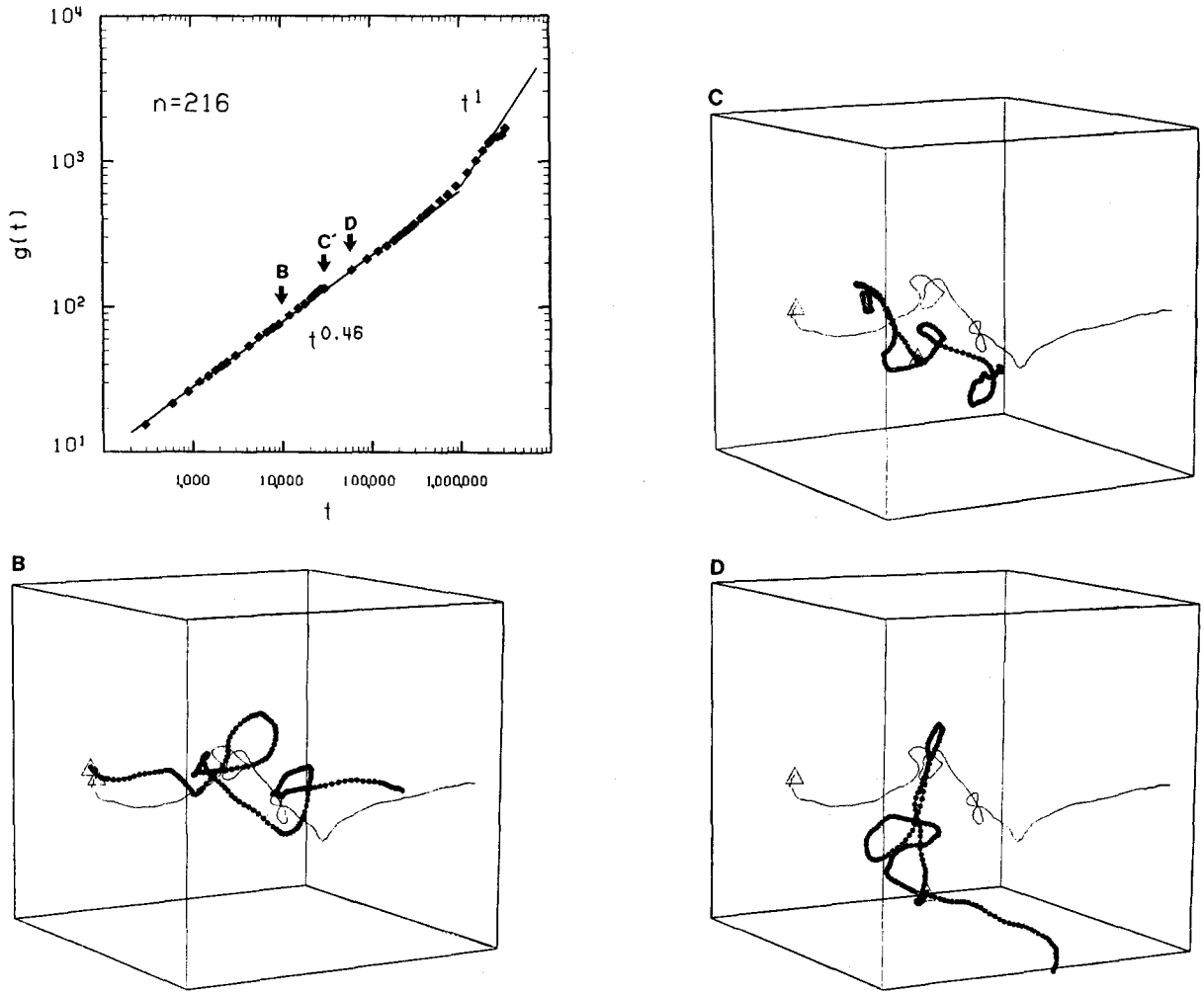

FIG. 18. Log–log plot of $g(t)$ vs t. (A) The arrows denote the time intervals, Δt, between snapshots of the original primitive path at $t_0 = 0$ (solid line) and the primitive path at a time Δt later (solid circles) shown in Figs. 18(B)–18(D). (B) $\Delta t = 10^4$; (C) $\Delta t = 3\times 10^4$; (D) $\Delta t = 5\times 10^4$. In all cases $n = 216$ and $\phi = 0.5$. In (B)–(D), the triangle locates the position of one of the chain ends.

required to obtain free diffusive motion [i.e., where $g_{\text{c.m.}}(t) \simeq 2\langle S^2\rangle$]. Hence, since the times are short compared to the tube renewal time in the reptation model, reptation, if it were occurring in our model system, should be observed.[1–6,32–34]

Thus, in the melt where all chains are moving, we see no evidence of a tube or reptation. The possibility of course exists that these chains are too short to see reptation; it has been conjectured that static and dynamic entanglement lengths are not the same[11,13] (however the notion of a dynamic entanglement remains ill defined, and as yet has not been put on a quantitative basis). Even conceding this possibility, we must still contend with the fact that the $\phi = 0.75$ system exhibits the behavior $D \sim n^{-2}$ and $\tau_R \sim n^{3.4}$ required by experiment. Therefore, the molecular weight dependence of D and/or τ_R alone cannot be used as the basis for the proof of reptation. Rather, these simulations suggest that at a minimum there should be a broad crossover regime from ideal Rouse behavior (with $D \sim n^{-1}$, $\tau \sim n^2$) in which lateral fluctuations of the chain are very important and in which reptation is at best a minor component of the motion.

E. Motion of a chain in a partially frozen environment

In order to check the observation that the large fluctuations of topological constraints in the model polymer melt are responsible for the lack of reptation, following previous workers[27–29,35] we performed a relatively short-time simulation of the motion of a single mobile polymer chain in a partially frozen matrix. (It should be mentioned that using a completely frozen matrix leads to a grid-locked system with no globally mobile chains at the density $\phi = 0.5$ considered. Whether the completely frozen matrix would allow for single mobile chain motion at times substantially longer than those run we cannot say. Nor can we exclude the possibility that if a large ensemble were examined, a certain fraction of chains would undergo global motion.) The model is schematically depicted in Fig. 20. All the chains, but one, have been partially frozen. Namely, we pinned the matrix chains every $n_e = 18$ beads for the two sets of chain lengths $n = 100$, and $n = 216$ at $\phi = 0.5$. Thus, there are 6 pinned beads for chains of $n = 100$, and 12 pinned beads for chains of $n = 216$. Oth-

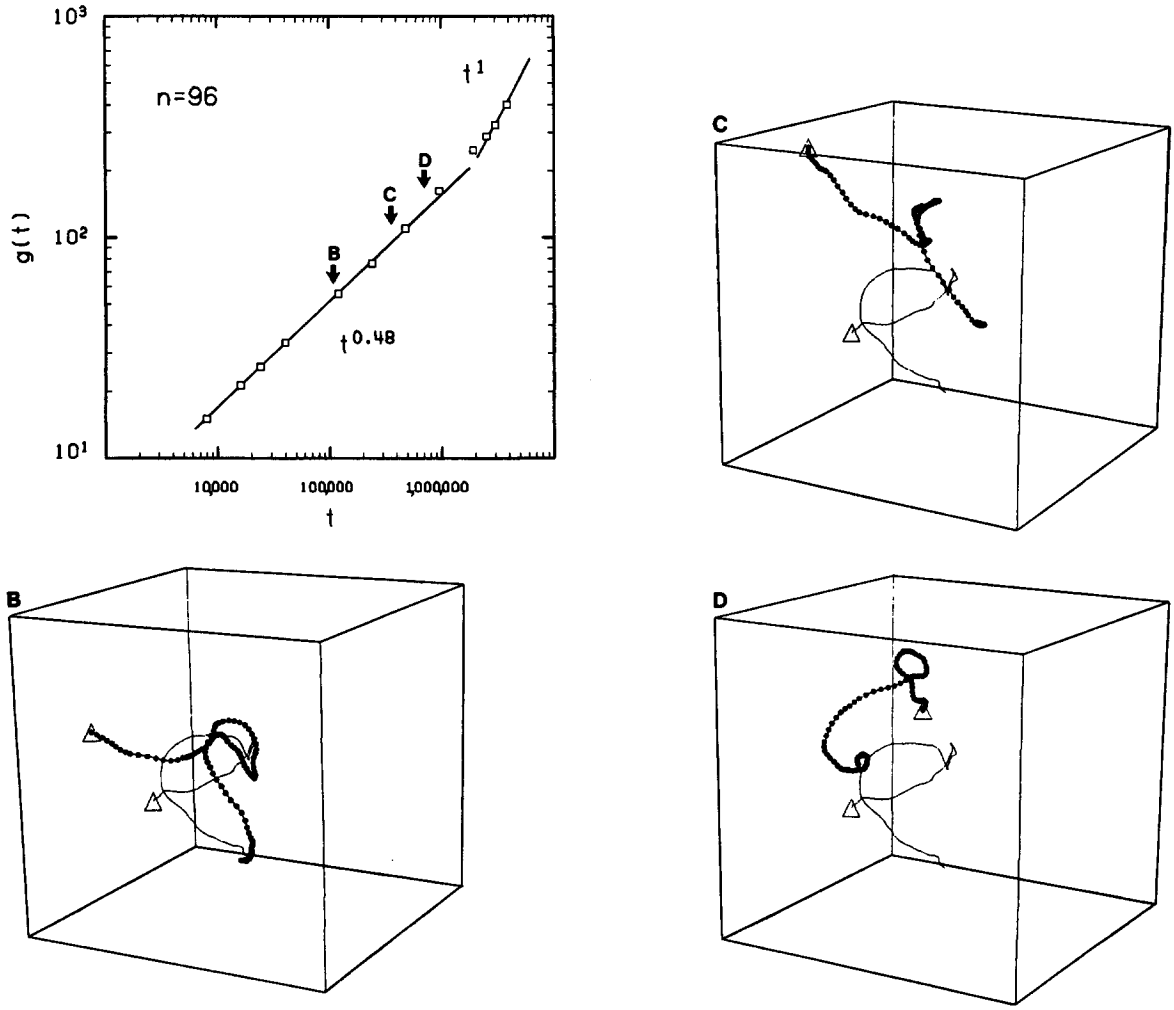

FIG. 19. Log–log plot of $g(t)$ vs t. (A) The arrows denote the values of the time invervals Δt between snapshots of the original primitive path at $t_0 = 0$ (solid line) and the primitive path at a time Δt later (solid circles) shown in Figs. 19(B)–19(D). (B) $\Delta t = 1.2\times10^5$; (C) $\Delta t = 3.6\times10^5$; (D) $\Delta t = 7.2\times10^5$. In all cases, $n = 96$ and $\phi = 0.75$. In (B)–(D), the triangle locates the position of one of the chain ends.

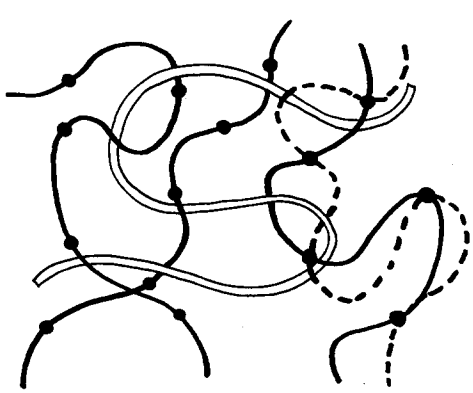

FIG. 20. Schematic representation of a single mobile chain represented by the open lines in a partially frozen environment of chains (solid lines). The solid circles denote locations at which the matrix chains are fixed. The dashed line shows some allowed fluctuations of a matrix chain consistent with the constraint that the pinned points cannot move. For ease of visualization, only one matrix chain is drawn as moving between pinned beads; however, in the MC simulation, all the matrix chains are allowed to move between pinned beads.

erwise the dynamics of all of the chains is modeled in exactly the same way as in the melt simulation algorithm. The matrix chains between the pinned beads are free to move as far as chain connectivity allows. This series of simulations allows us to demonstrate that (1) reptation is not artificially suppressed by confining the single test polymer to a lattice. (2) The equivalent path analysis gives $g_\perp(t)/g_\parallel(t)$ and primitive path trajectories in agreement with the expected behavior for reptating chains. Namely, $g_\perp(t)/g_\parallel(t)$ monotonically decreases with time and tube memory effects are evident.

For the case of a single chain in the partially frozen environment described above we obtain results consistent with the reptation picture. In Fig. 21, a log–log plot of the single bead autocorrelation function vs time is presented for the cases of a single mobile chain with $n = 100$ and 216, both at $\phi = 0.5$, in the curves represented by open triangles and solid diamonds, respectively. There is clearly a crossover from the initial $g(t) \sim t^{1/2}$ regime to a regime of slower motion, consistent with $g(t) \sim t^{1/4}$, reflecting the motion of the

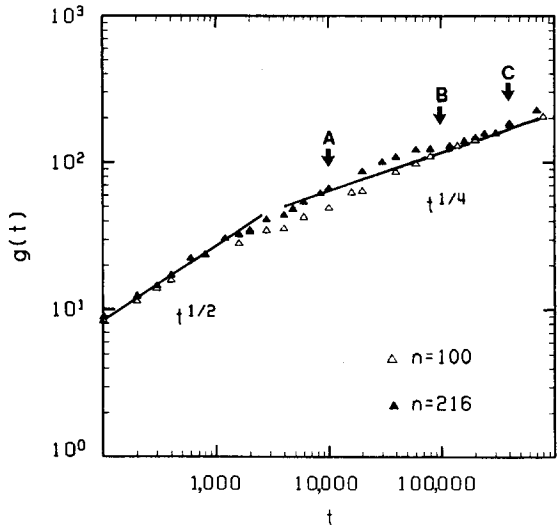

FIG. 21. Log–log plot of $g(t)$ vs t for the single mobile chain in a partially frozen matrix of chains, all packed at an overall density $\phi = 0.5$. $n = 100$ and 216 in the open and solid triangles, respectively. The arrows denote the time intervals between snapshots of the original primitive path defined at $t_0 = 0$, and a snapshot at time Δt later for the $n = 216$ chain shown in Figs. 22(A)–22(C).

chain along the tube.[1,2] The crossover at $30 < g(t) < 80$ gives the tube diameter $d_T \cong 6$ which is consistent with the superimposed restrictions on the mobility of the matrix chains. Furthermore, the ratio of $g_\perp(t)/g_\parallel(t)$ for the $n = 216$ chain at $\phi = 0.5$ in a partially frozen environment, as shown in the curve drawn through the solid diamonds in Fig. 17, decreases with increasing time. If pure reptation were occurring, it would decay essentially to zero. However, as evidenced by the snapshots shown in Figs. 22(A)–22(C) at various time intervals between the equivalent paths, there is quite a lot of tube leakage[6] (there cannot be constraint release since the environment is permanently pinned) which slows down the dynamics relative to the pure reptation case. That is, the mobile chain spends a lot of time running up and down cul-de-sacs. This points out that tube leakage may be an important mechanism in those systems such as polymer chains in a gel that have been shown to reptate.[63]

IV. DISCUSSION

The behavior of the diamond lattice multichain systems we studied is qualitatively consistent with the experimental results for polymer melts.[14,15] Namely, at a density of $\phi = 0.75$, $D \sim n^{-2.1}$ and $\tau_R \sim n^{3.4}$. As the density is lowered, there is a smooth crossover to $D \sim n^{1.15}$ and $\tau_R \sim n^{2.35}$ for an isolated single chain with excluded volume interactions. At first glance the results at high density for D and τ_R are apparently consistent with the reptation model.[1–6] However, an analysis of the single bead motion as well as an analysis of the "primitive path" migration shows that the dynamics is really closer to that of a Rouse chain[9] in that lateral fluctuations are important, and there is apparently no tube for the range of n studied. These simulations indicate that the notion of static constraints seems to be irrelevant to the motion of a given chain, if all of the chains are mobile. However, the motion of the system significantly slows down as the concentration increases and cooperativity of motion between chains becomes evident. Eventually at some critical density, ϕ_G, $D = 0$, and only local fluctuations persist. The vanishing of D is caused by the increase of the local friction constant, which seems to be well described by a simple free volume treatment.

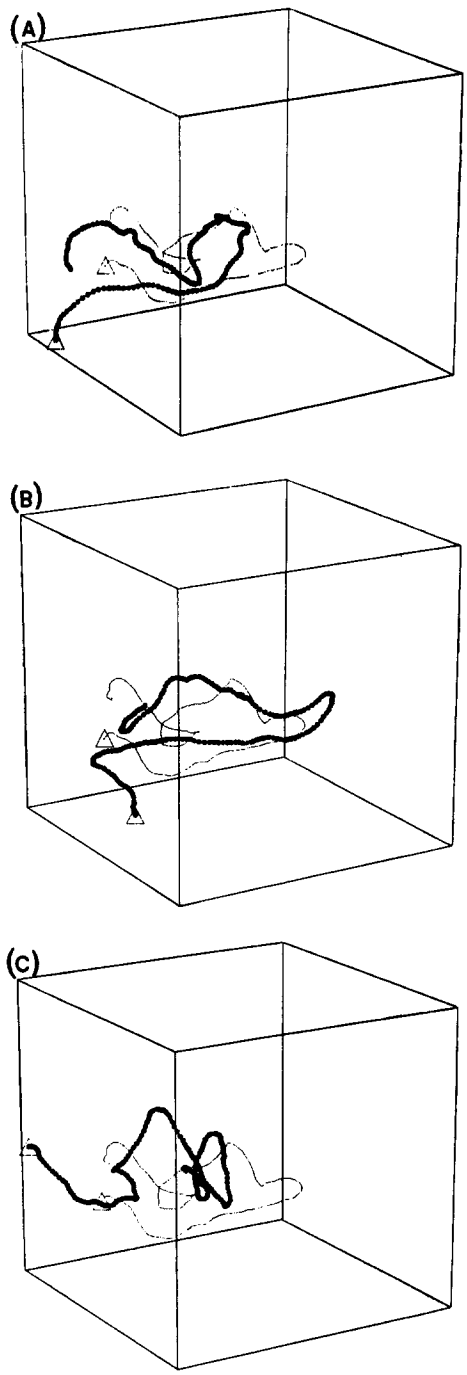

FIG. 22. For a single mobile chain in a partially frozen environment, snapshots of primitive paths separated by (A) $\Delta t = 10^4$, (B) $\Delta t = 10^5$, and (C) $\Delta t = 4 \times 10^5$, respectively. In all cases $n = 216$, and $\phi = 0.5$. In (A)–(C), the triangle locates the position of one of the chain ends.

Finally, the question arises if our result that $\tau_R \sim n^{3.4}$ is caused by the suppression of conformation-changing elementary four-bond jumps. This is not the case for the following two reasons. First, we have shown in previous work[8] that

four-bond jumps are shutdown at ϕ_G, but not below this density, and the dynamical properties of the system are not sensitive to the particular *a priori* choice of the ratio of three-bond to four-bond motions.[8,13] Hence, there are still substantial possibilities to create new orientations in the middle part of the chain and therefore the n^3 scale is not built into the model. On the contrary, considerable internal reorientation is seen for times much shorter than τ_R. Second, as was also shown previously,[8] the *a priori* exclusion of four-bond motions at densities much lower than ϕ_G leads to $D = 0$. The relatively long polymers studied here exhibit unconstrained dynamics and only very short polymers ($n \leqslant 36$) are sensitive to the details of the elemental dynamics (i.e., the *a priori* ratio of three-bond motions to four-bond motions). For these shorter chains, the scaling exponents in the chain length dependence of τ_R and D are slightly dependent on the local dynamic parameters of the model. For longer chains, changing the value of the *a priori* probabilities of three- and four-bond jumps simply leads to rescaling the time unit by a constant factor.

Having only a discrete set of elementary motions, a discrete representation of the polymer conformations, and a discrete distribution of free volume are intrinsic disadvantages of lattice models. But again, these efffects should be screened out after a short distance and therefore only produce a linear change of the time scale, if the polymer is long enough. Indeed, we find agreement in the qualitative behavior seen here with that of off-lattice simulations.[35]

The above limitations of the lattice representation, which primarily affect short polymers, may be the reason why we have not observed the crossover region discussed above from the $D \sim n^{-1}$ to $D \sim n^{-2}$, and the $\tau_R \sim n^{2.2}$ to $\tau_R \sim n^{3.4}$ behavior with increasing chain length. On other hand, a polymer having $n = 12$ in our model system is comparable to a real polymer with degree of polymerization that is several times larger and may be quite close to the critical chain length seen in viscosity measurements. Since lattice dynamics becomes less and less physical as the chain length decreases, we have not attempted to check for a crossover regime and have not simulated chains with $n < 12$.

V. CONCLUSIONS

Using a dynamic MC simulation of a dense diamond lattice system of entangled chains, we have shown that reptation within a tube is not a necessary condition to observe $D \sim n^{2.1}$ and $\tau_R \sim n^{3.4}$. Rather, this simulation argues for the existence of a regime where there is considerable lateral motion of a chain to achieve long distance displacements and where there is no evidence whatsoever for the existence of a tube. Indeed, reptation-like behavior is observed only when we partially freeze the environment surrounding the chain of interest by pinning the other chains. Thus we are led to the conclusion that reptation is the dominant mode of diffusive behavior for these finite length chains only when the polymer is in an environment with a markedly slower time scale of motion—such as a polymer in a crosslinked gel. In a melt or concentrated solution where there is no separation of time scales between the chain of interest and the other surrounding chains, the polymer behaves much more like the classical Rouse chain with the caveats noted below. Thus, while we cannot rule out the possibility that reptation becomes the dominant mode of relaxation in the limit of very high molecular weight, at the very least, these simulations strongly argue for the existence of a crossover regime between simple Rouse behavior and reptation, where reptation is an unimportant component of the mechanism of the long distance displacement of a chain in the melt. This crossover regime exhibits $D \sim n^{-2}$ and $\tau_R \sim n^{3.4}$ but has dynamic properties quite different from those described by reptation theory. An analytic theory capable of describing the dynamics of chains in this regime does not, at present exist.

Qualitatively, the behavior of the chains is closest to the Rouse model in that the large distance motion is essentially isotropic with no evidence of tube memory effects.[9] The single bead autocorrelation function $g(t)$ also possesses a $t^{1/2}$ (actually $t^{0.46}$) regime as does the Rouse model in the large n limit; however, the sharpness of the crossover from the $t^{1/2}$ to the t^1 regime at the finite n studied in the simulation are not reproduced by the Rouse model. Moreover, $g_{\text{c.m.}}(t) \sim t^{0.9}$ for mean-square displacements $\leqslant 2\langle S^2 \rangle$, after which free diffusive behavior takes over. A pure Rouse model requires $g_{\text{c.m.}}(t) \sim t$ at all times. Furthermore, the chain ends are more mobile than is predicted from a Rouse model with a uniform bead friction constant. Thus, while the behavior of the entangled melt of chains is much closer to a Rouse chain

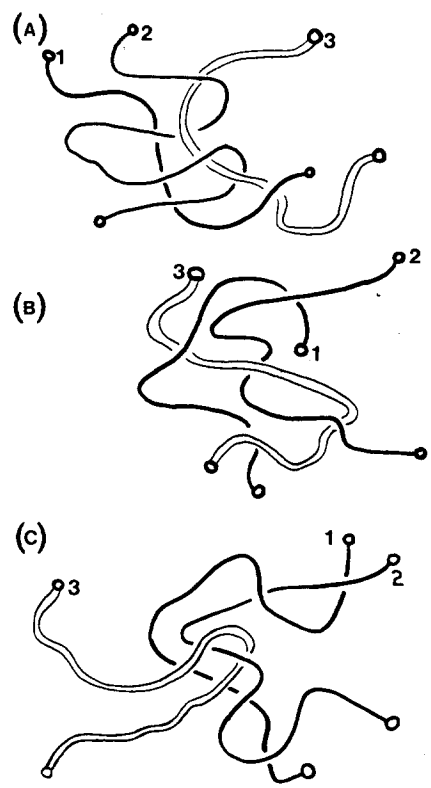

FIG. 23. Schematic representation of a possible mechanism of motion of polymer chains in the melt in which there is a cooperative flow between neighbors that allows the chains shown in Fig. 23(A) to interchange relative positions as shown in Fig. 23(C). (A) Representation of possible mechanism of motion of polymer chains. (B) An intermediate state is shown in Fig. 23(B). (C) Chains from Fig. 23(A) interchange relative positions.

than to a reptating chain, the Rouse characterization is only approximate and fails to capture some essential features of the melt dynamics.

The physical picture of the diffusive motion of the polymer chains in a melt that emerges from this study is that the chains move in a random fashion in some sense similar to the motions responsible for polymer diffusion in dilute solution. However, the motions of the various chains are highly cooperative. As one polymer diffuses, we conjecture that there is a backflow of the surrounding polymer chains. This backflow is necessary in order to conserve local density. It is this concerted backflow motion which leads to the much larger chain length dependence of diffusion and viscosity for concentrated polymer systems than is observed in dilute solution. A schematic zero order picture of one such cooperative mutual flow process is given in Figs. 23(A)–23(D) where the chain of interest, chain three, flows past chains one and two, in a "push-me/pull-you" fashion.

In future work, we shall extend our study to longer chains, examine the dynamics of a smaller chain in a larger molecular weight matrix, and explore the dynamics of a chain in a microgel. All these studies are designed to qualitatively elucidate the behavior of multichain systems and to form the basis of new analytic theories of melt dynamics that these simulations strongly suggest are required.

Note Added in Proof: We recently completed a MC simulation of cubic lattice chains packed at $\varphi = 0.5$ over a range of $n = 64,100,216$, and 800. For the entire range of n studied, including the $n = 800$ chains, identical qualitative results as those described here were seen. Moreover, simulations of smaller chains in a matrix of larger chains are in qualitative agreement with experiment,[24,25] and yet no evidence for reptation as the dominant mode of melt motion was found. Manuscripts describing the more recent work are now in preparation.

ACKNOWLEDGMENTS

This research was supported in part by a grant from the Polymer Program of the National Science Foundation (No. DMR-85-20789). Acknowledgment is made to the Monsanto Company for an institutional research grant for the purchase of two μVAX-II computers on which the simulations reported here were predominantly carried out. Useful discussions with K. Binder, M. Doi, W. Graessley, E. Kramer, K. Kremer, M. Rubinstein, W. H. Stockmayer, H. Yu, and B. H. Zimm are gratefully acknowledged.

APPENDIX: ESTIMATION OF THE NUMBER OF KNOTS

One way to estimate the number of knots is to fix the ends of all the chains, and in the off-lattice case, reel in the slack and then count the resulting number of kinks.[62] Chains having conformations such as shown in Figs. 24(A) and 24(B) are reduced to straight lines by this procedure and thus lack knots. On the other hand, chains 1, 3, and 4 of Fig. 24(C) possess one kink each, and chain 2 possesses three kinks; these are counted as intermolecular entanglements. The single chain shown in Fig. 24(D) possesses one "true" knot, but since self-entanglements are in some sense irrelevant to the problem of mutual diffusion of the chains, these knots have to be subtracted out.

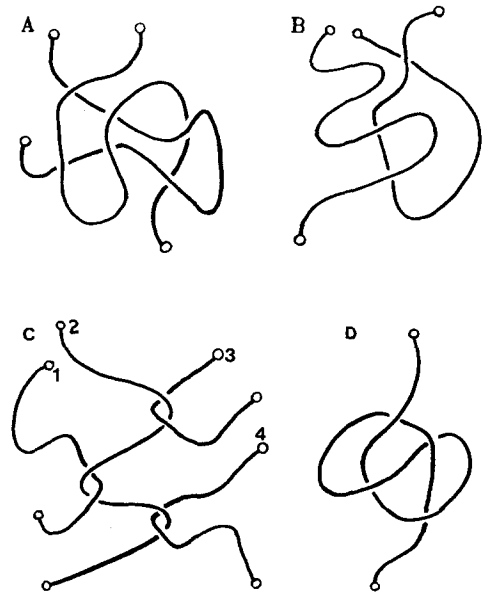

FIG. 24. Schematic illustration of the kinds of conformations considered in the knot counting algorithm. (A) Two conformations of chains that do not give rise to knots when subjected to the chain end pulling algorithm described in the Appendix. (B) Same as (A). (C) Schematic conformation of chains that gives rise to knots when subjected to the chain end pulling algorithm described in the Appendix. (D) An example of a self-entanglement which does not contribute to the number of interchain knots when subjected to the pulling algorithm described in the Appendix.

Unfortunately, when chains are confined to a lattice the pulling process becomes more complicated since these chains also possess a number of kinks due entirely to lattice constraints. Thus, the knot counting process is realized as follows: First, the chain is reduced to an fcc lattice by neglecting every second bead, a process which never violates the requirement that two bonds cannot cross. Then, to obtain the average number of kinks equivalent to a straight line segment, the prohibition against multiple occupancy of sites belonging to beads on different chains is removed, thus producing a collection of N noninteracting chains. An iterative pseudorandom process is used to search for the shortest possible fcc-lattice path between the two chain ends, taking into consideration the intrachain topological constraints. The above procedure leads to a reduction in chain contour length and allows as to estimate the average number of kinks, n_k^0 equivalent to a straight segment. We then repeat the procedure for the N chains in which the multiple occupancy exclusion of lattice sites applicable to all beads is restored. The iterative pseudorandom process described above is then applied to the collection of chains in the melt, giving the average number of kinks in the melt n_{mk}. If the true entanglement points are sufficiently far apart, we can assume that each equivalent line segment contains n_k^0 kinks; that is, equivalent straight line segments in the two cases (with and without intermolecular excluded volume) are self-similar. Therefore a lower bound for the number of entanglements or knots is the ratio n_{mk}/n_k^0. This number is reported in row four of Table IV.

[1] P. G. de Gennes, Phys. Today **36**, No. 6, 33 (1983).
[2] P. G. de Gennes, *Scaling Concepts in Polymer Physics* (Cornell University, Ithaca, New York, 1979).

[3]P. G. de Gennes, J. Chem. Phys. **55**, 572 (1971).
[4]M. Doi and S. F. Edwards, J. Chem. Soc. Faraday Trans. 2 **74**, 1789, 1802, 1818 (1978); **75**, 38 (1978).
[5]W. W. Graessley, J. Polym. Sci. Polym. Phys. Ed. **18**, 27 (1980).
[6]W. W. Graessley, Adv. Polym. Sci. **16**, 1 (1974); **47**, 67 (1982).
[7]A recent review of dynamic Monte Carlo simulations for polymer systems with references to earlier work is A. Baumgartner, Annu. Rev. Phys. Chem. **35**, 419 (1984).
[8]A. Kolinski, J. Skolnick, and R. Yaris, J. Chem. Phys. **84**, 1922 (1986).
[9]P. E. Rouse, J. Chem. Phys. **21**, 1272 (1953).
[10]See for example, R. N. Haward, *The Physics of Glassy Polymers* (Wiley, New York, 1973).
[11]A. Baumgartner, J. Chem. Phys. **73**, 2489 (1980).
[12]R. D. Batie, J. L. Viovy, and L. Monnerie, J. Chem. Phys. **81**, 567 (1984).
[13]K. Kremer, Macromolecules **16**, 1632 (1983).
[14]G. C. Berry and T. G. Fox, Adv. Polym. Sci. **5**, 261 (1968).
[15]J. D. Ferry, *Viscoelastic Properties of Polymers* (Wiley, New York, 1980).
[16]J. Klein, Nature **271**, 143 (1978).
[17]R. Kimmich and R. Bachus, Colloid. Polym. Sci. **260**, 586 (1982); Polymer **24**, 964 (1983).
[18]G. Fleischer, Polym. Bull. Berlin **152**, 9 (1983); **11**, 75 (1984).
[19]J. Klein, D. Fletcher, and L. J. Fetters, Nature (London) **304**, 526 (1983).
[20]C. R. Bartels, B. Crist, and W. W. Graessley, Macromolecules **17**, 270 (1984).
[21]J. A. Wesson, I. Noh, T. Kitano, and H. Yu, Macromolecules **17**, 782 (1984).
[22]P. F. Green, C. J. Palmstrom, J. W. Mayer, and E. J. Kramer, Macromolecules **18**, 501 (1985).
[23]P. F. Green, P. J. Mills, C. J. Palmstrom, J. W. Mayer, and E. J. Kramer, Phys. Rev. Lett. **53**, 2145 (1984).
[24]M. A. Antonietti, J. Coutandin, and H. Sillescu, Macromolecules **19**, 793 (1986).
[25]P. F. Green and E. J. Kramer, Macromolecules **19**, 1108 (1986).
[26]H. Yamakawa, *Modern Theory of Polymer Solutions* (Harper and Row, New York, 1969), Chap. VI.
[27]K. E. Evans and S. F. Edwards, J. Chem. Soc. Faraday Trans. 2 **77**, 1891, 1929 (1981).
[28]S. F. Edwards and K. E. Evans, J. Chem. Soc. Faraday Trans. 2 **77**, 1913 (1981).
[29]A. Baumgartner and K. Binder, J. Chem. Phys. **75**, 2994 (1981).
[30]M. Doi, J. Polym. Sci. Polym. Lett. Ed. **19**, 265 (1981).
[31]R. J. Needs, Macromolecules **17**, 437 (1984).
[32]J. Klein, Macromolecules **11**, 852 (1978).
[33]J. Klein, Macromolecules **19**, 105 (1986).
[34]M. Daoud and P. G. de Gennes, J. Polym. Sci. Polym. Phys. Ed. **17**, 1971 (1979).
[35]See for example, M. Bishop, D. Ceperley, H. L. Frisch, and M. H. Kalos, J. Chem. Phys. **76**, 1557 (1982).
[36]S. F. Edwards, Polymer **6**, 143 (1977).
[37]P. H. Verdier and W. H. Stockmayer, J. Chem. Phys. **36**, 227 (1962).
[38]K. Iwata and M. Kurata, J. Chem. Phys. **50**, 4008 (1969).
[39]R. A. Orwoll and W. H. Stockmayer, Adv. Chem. Phys. **15**, 305 (1969).
[40]D. E. Kranbuehl and P. H. Verdier, J. Chem. Phys. **71**, 2662 (1979), and references cited therein.
[41]D. E. Kranbuehl and P. H. Verdier, J. Chem. Phys. **67**, 361 (1977).
[42]H. J. Hilhorst and J. M. Deutch, J. Chem. Phys. **63**, 5153 (1975).
[43]H. Boots and J. M. Deutch, J. Chem. Phys. **67**, 4608 (1977).
[44]M. T. Gurler, C. C. Crabb, D. M. Dahlin, and J. Kovac, Macromolecules **16**, 398 (1983).
[45]C. Stokely, C. C. Crabb, and J. Kovac, Macromolecules **19**, 860 (1986).
[46]F. Geny and L. Monnerie, J. Polym. Sci. Polym. Phys. Ed. **17**, 131, 147 (1979).
[47]K. Kremer, A. Baumgartner, and K. Binder, J. Phys. A **15**, 2879 (1981).
[48]K. Iwata and M. Kurata, J. Chem. Phys. **59**, 6119 (1973).
[49]P. J. Flory, *Statistical Mechanics of Chain Molecules* (Interscience, New York, 1969).
[50]F. T. Wall and W. A. Seitz, J. Chem. Phys. **67**, 3722 (1977).
[51]J. G. Curro, J. Chem. Phys. **12**, 463 (1979).
[52]C. Domb and M. E. Fisher, Proc. Cambridge Philos. Soc. **54**, 48 (1958).
[53]P. G. de Gennes, Macromolecules **9**, 587 (1976).
[54]M. Dial, K. S. Crabb, C. C. Crabb, and J. Kovac, Macromolecules **18**, 2215 (1985).
[55]C. C. Crabb and J. Kovac, Macromolecules **18**, 1430 (1985).
[56]D. E. Kranbuehl and P. H. Verdier, Macromolecules **17**, 749 (1984).
[57]N. Nemoto, M. R. Landry, I. Noh, T. Kitano, J. A. Wesson, and H. Yu, Macromolecules **18**, 308 (1985).
[58]D. W. Schaefer, Polym. Prepr. Am. Chem. Soc. Div. Polym. Chem. **23**, 53 (1982).
[59]Reference 15, p. 489.
[60]A. S. Marshall and S. E. B. Petrie, J. Appl. Phys. **46**, 42 (1975).
[61]A. Kolinski, J. Skolnick, and R. Yaris, Macromolecules **16**, 2560 (1986). (in press).
[62]M. Rubinstein and E. Helfand, J. Chem. Phys. **82**, 2477 (1985).
[63]O. Lumpkin and B. H. Zimm, Biopolymers **24**, 1573 (1985), and references cited therein.